united nations educational, scientific and cultural organization

international atomic energy agency

the
abdus salam
international centre for theoretical physics

SMR 1273 - 6

WORKSHOP ON PLASMA DIAGNOSTICS AND INDUSTRIAL APPLICATIONS OF PLASMAS

12 - 13 OCTOBER 2000

INDUSTRIAL APPLICATIONS OF SMALL PLASMA DEVISES AND RELATED DIAGNOSTICS

Part II

Jorge FEUGEAS
Rosario Institute of Physics (IFIR)
Bv. 27 de Febrero 210 Bis.
2000 Rosario, Argentina

These are preliminary lecture notes, intended only for distribution to participants.

INDUSTRIAL APPLICATIONS OF SMALL PLASMA DEVISES AND RELATED DIAGNOSTICS

Jorge Feugeas

Surface Engineering Laboratory

Rosario Institute of Physics

National Council of Research-University of Rosario

(Interinstitutional Program of Dense Plasmas)

Jorge Feugeas

- PhD in Physics (Stevens Ins[illegible] Tecnology, USA)
- Professor, University of Rosario (Experimental Phys.)
- Researcher, National Council of Research
- Vice Director of the Rosario Institute of Physics
- President of ACIFIR Foundation (Transference of Technology Institution)

- <u>Address</u>: IFIR, Bv. 27 de Febrero 210 Bis. 2000 Rosario, Argentina
- e-mail: feugeas@ifir.ifir.edu.ar

GROUP OF RESE

- **Jorge Feugeas, PhD**
  (Researcher, Group Director)
- **Bernardo Gómez, PhD**
  (Researcher, Laboratory / Enterprise)
- **Aldo Marenzana, Electrical Engineer**
  (Graduate Student (PhD), Laboratory)
- **Lucas Nachez, Licenciado in Physics**
  (Graduate Student (PhD), Laboratory)
- **HoracioMerayo**
  (Technician, Laboratory)
- **Andrés Devooght**
  (Technician, Enterprise)

FINANTIAL SUP

GRANTS (Today)

- National Council of Research (CONIC
- Secretary of Science and Technology
- International Atomic Energy Agency (IAEA)
- University of Rosario

GRANTS (Past)

- ICTP-TWAS, Trieste (Italy)
- Antorchas Foundation (Argentina)
- Vitae Foundation (Brazil)
- Fulbright Foundation (U.S.A)

OTHER SUPPORTS

- Inter-institutional Program of Dense Plasmas (Argentina)
- Enterprise Galplast S.R.L. (Rosario, Argentina)

COLLABORATION WITH OTHER GROUPS OF RESEARCH

IN ARGENTINA

- National Atomic Energy Comission (CNEA)
- Argentine Institute of Siderurgy (IAS), San Nicolas
- Institute of Technology (INTEC), Santa Fe
- CITEFA, Buenos Aires

OTHER COUNTRIES

- National Laboratory of Synchrotron Radiation (LNLS), Campinas, Brazil
- COPPE, Rio de Janeiro, Brazil
- Escola de Minas, Ouro Preto, Brazil
- Universite Paul Sabatier, Toulouse, France
- Laboratoire de Mécanique de Lille, URA, CNRS, Lille, France

FIELD OF RESEARCH: "Surface treatment by means of techniques that use plasmas"

HIGH ENERGY PLASMAS

- Surface treatment by thermal shock.

High energy, short duration pulses of plasmas generated in Z-Pinch experiments.

[illegible] TEMPERATURE PLASMAS

- Ion nitriding
- Ion nitrocarburizing
- Plasma Assisted Physical Vapor Deposition

DC and pulsed Glow discharges, combined with pure metal evaporation.

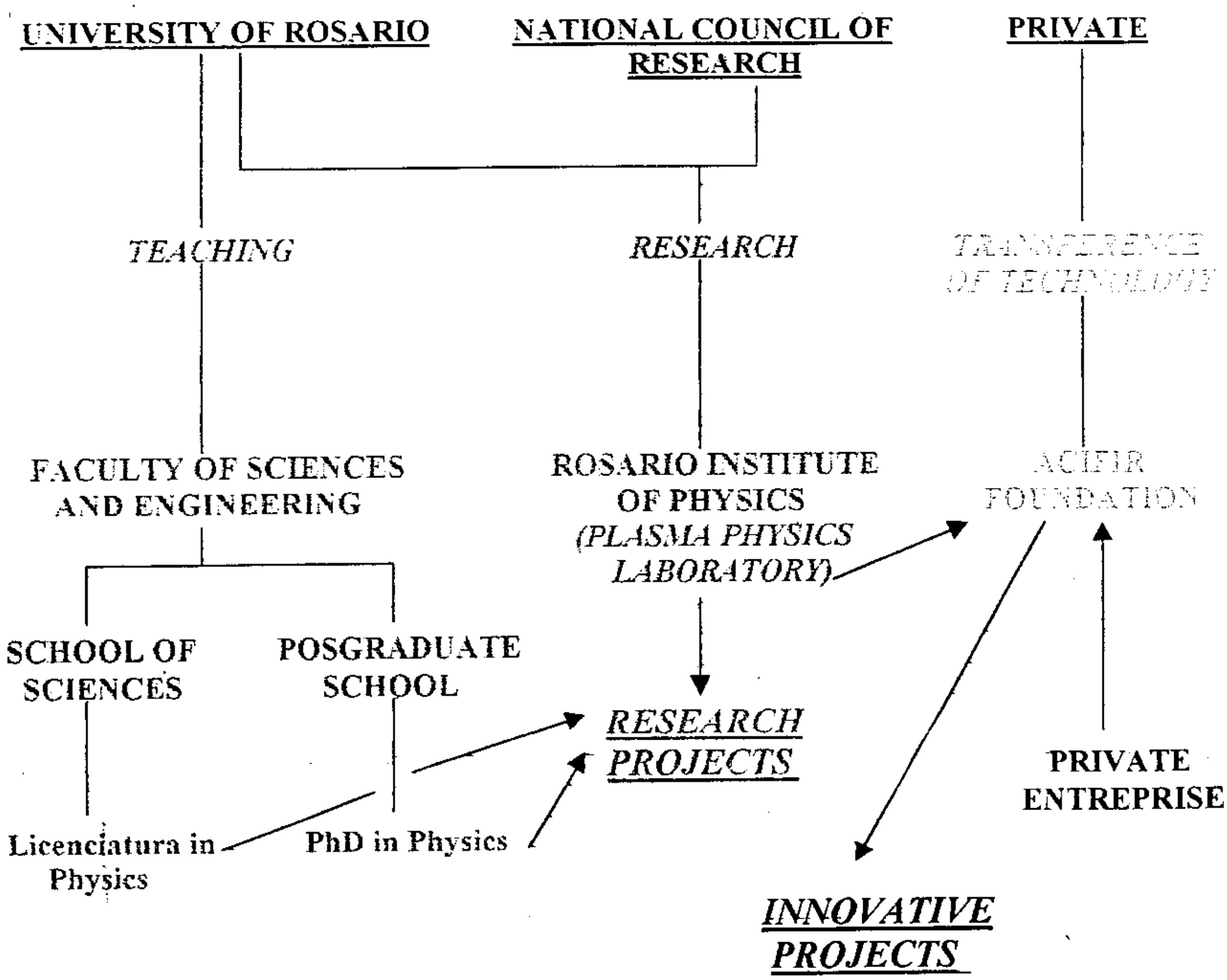
UNIVERSITY OF ROSARIO
NATIONAL COUNCIL OF RESEARCH
PRIVATE
TEACHING
RESEARCH
TRANSFERENCE OF TECHNOLOGY
FACULTY OF SCIENCES AND ENGINEERING
ROSARIO INSTITUTE OF PHYSICS (PLASMA PHYSICS LABORATORY)
ACIFIR FOUNDATION
SCHOOL OF SCIENCES
POSGRADUATE SCHOOL
RESEARCH PROJECTS
PRIVATE ENTREPRISE
Licenciatura in Physics
PhD in Physics
INNOVATIVE PROJECTS

CHARACTERISTICS OF THE PROJECT-ENTERPRISE

TYPE OF ENTERPRISE

- Small and medium size enterprises (<80 employees).
- Field of activity (manufacturing or services) with strong tradition in the region.
- Inserted in the internal and external (export) market.

This type of enterprises have strong dependence of the region.

Big companies in general buy new technology in developed countries.

CHARACTERISTICS OF THE PROJECTS

- Low investment.
- Short term benefits.
- Relatively short duration (<2 years)
- Possibility of active participation of part of the professionals and technicians of the enterprise.
- Mostly developed inside the enterprise (confidentiality).

ELEMENTS THAT HELP TO CAPT PROJECTS OF TRANSFERENCE OF TECHNOLOGY

- **Detection of the necessities of the en[illegible]**

It is more important to detect necessities [illegible] show to the managers the results of our research.

- **Helping to solve (directly or indirectly) any problems of the enterprises, even those that do not require an important professional (or intellectual) effort.**

This activity contributes to create confidence and break the concept of the existence of a strong gap between the small enterprise necessities and the creation of knowledge in the academic and scientific research groups.

- **Knowledge of possible financial help (credits, subsidies, etc.) available in financial market and from official institutions.**

This help to present realistic solutions even under the economic point of view.

- **To have a good knowledge of the state of the art of the application fields related with our specific field of research.**

PLASMA PHYSICS

Plasma physics is a discipline which [illegible] during the last 50 years. The effort [illegible] principally in nuclear fusion strongly push the research in many directions that left important knowledge that was fully used in many other applications. Methods of plasma production and diagnostic techniques were developed in abundance.

The strong exigency in quality in microelectronics also create an important number of sophisticated methods of surface treatment, mostly of them based on plasma physics, which were rapidly applied in other fields.

Today there are many applications in which plasma physics play an important role.

Many of the applications of plasma physics and the related diagnostic techniques are of relative low cost, making possible their development with modest budgets.

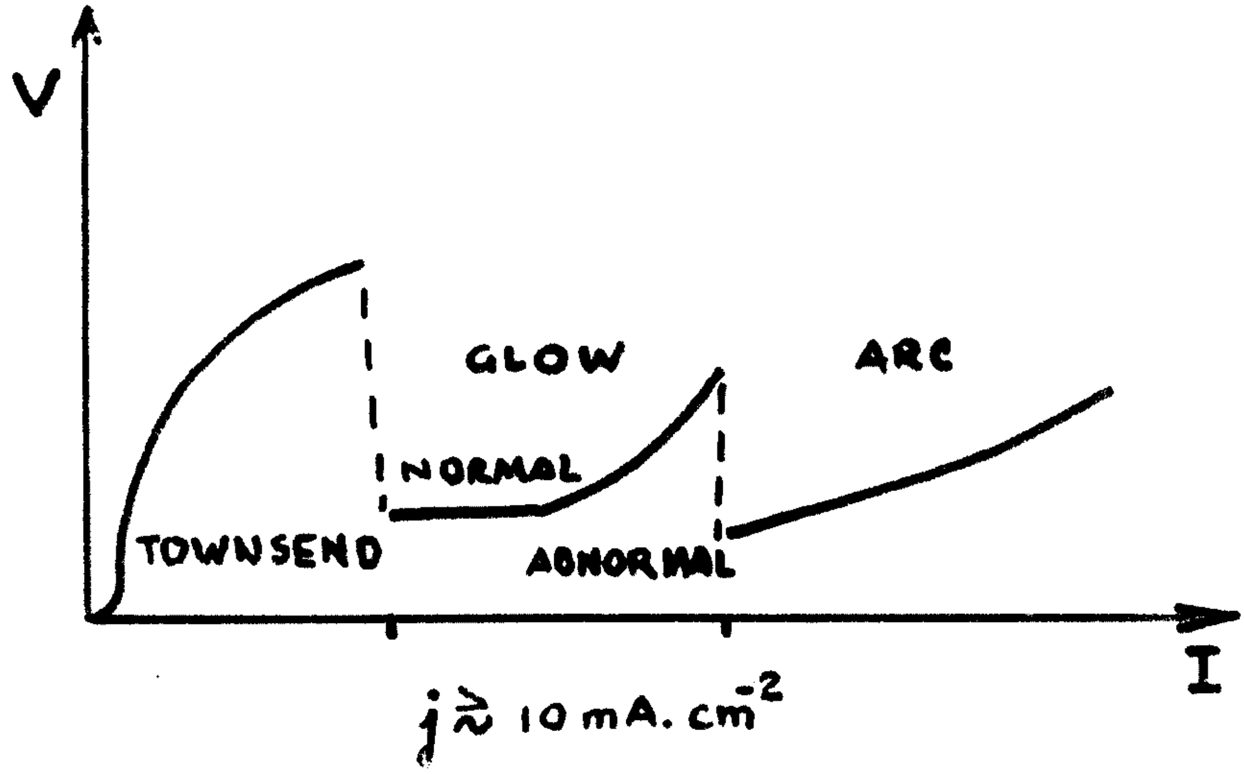
V
GLOW
ARC
NORMAL
TOWNSEND
ABNORMAL
I
j ≳ 10 mA.cm^-2

SOLAR FLARES

Annihilation of magnetic fields (Sweet's mechanism)

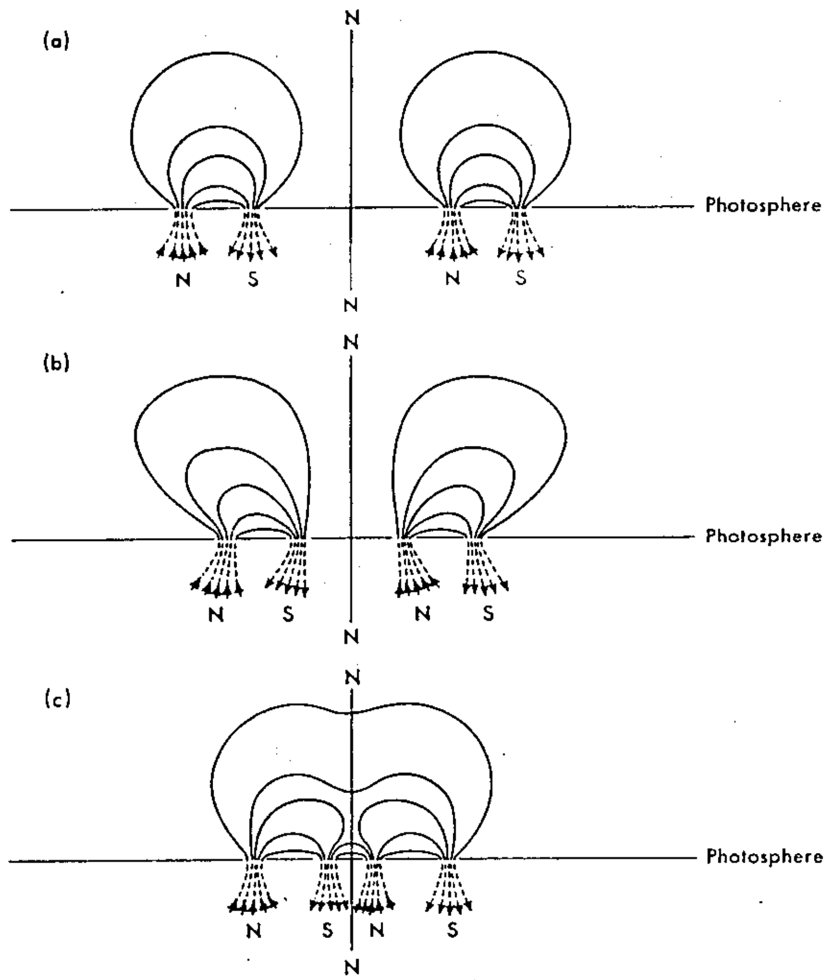

ION ACCELERATION DURING RAYLEIGH TAYLOR INSTABILITY (M=0) DEVELOPMENT, IN A HIGH CURRENT PLASMA COLUMN

A- PLASMA COLUMN

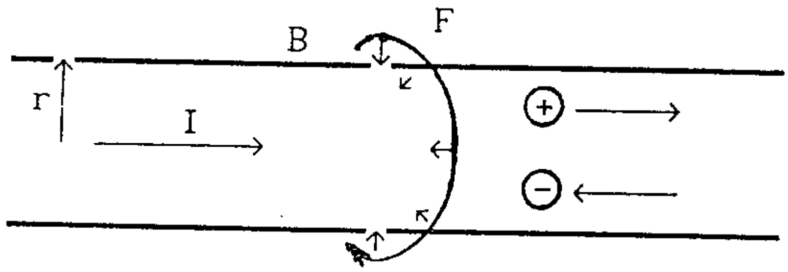

$B(t) \sim I(t)/r$

$F(t) \sim I(t) \times B(t)$

B- INSTABILITY DEVELOPMENT ("PINCH" EFFECT)

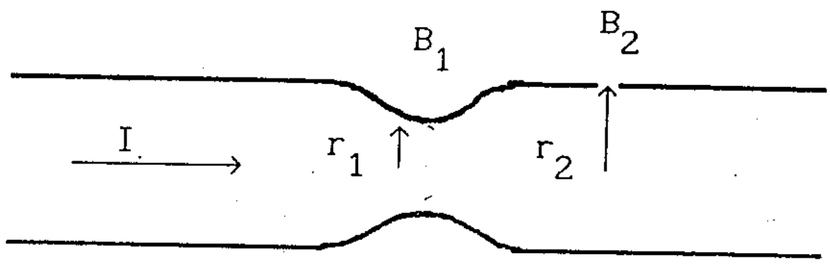

$F_1 \sim I \times B_1$

$F_2 \sim I \times B_2$

$F_1 > F_2$

C- DIODE LIKE FORMATION

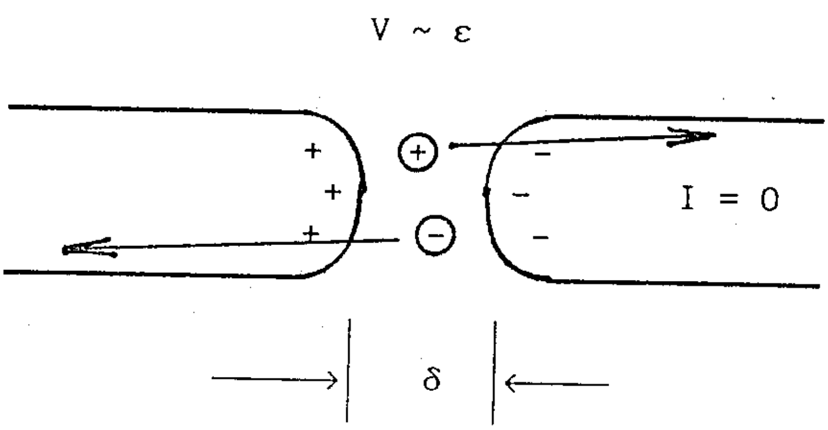

$\varepsilon = -\partial\Phi/\partial t$

$\varepsilon \sim \Delta(B.A)/\Delta t$

$B_i \sim I_i/\delta$

$B_f = 0$

$\varepsilon \sim (B_i.A)/\Delta t$

ESTIMATED FIELD

$\Delta I \sim I_m \sim 100kA$; $\Delta t \sim 0,1ns$; $A \sim \delta^2$; $\delta \sim 10\mu m$

$$\varepsilon \sim [\ (\mu_o I_m/2\pi\delta)\ .\ \delta^2\ ]\ /\ \Delta t$$

$$\varepsilon \sim 200\ kV$$

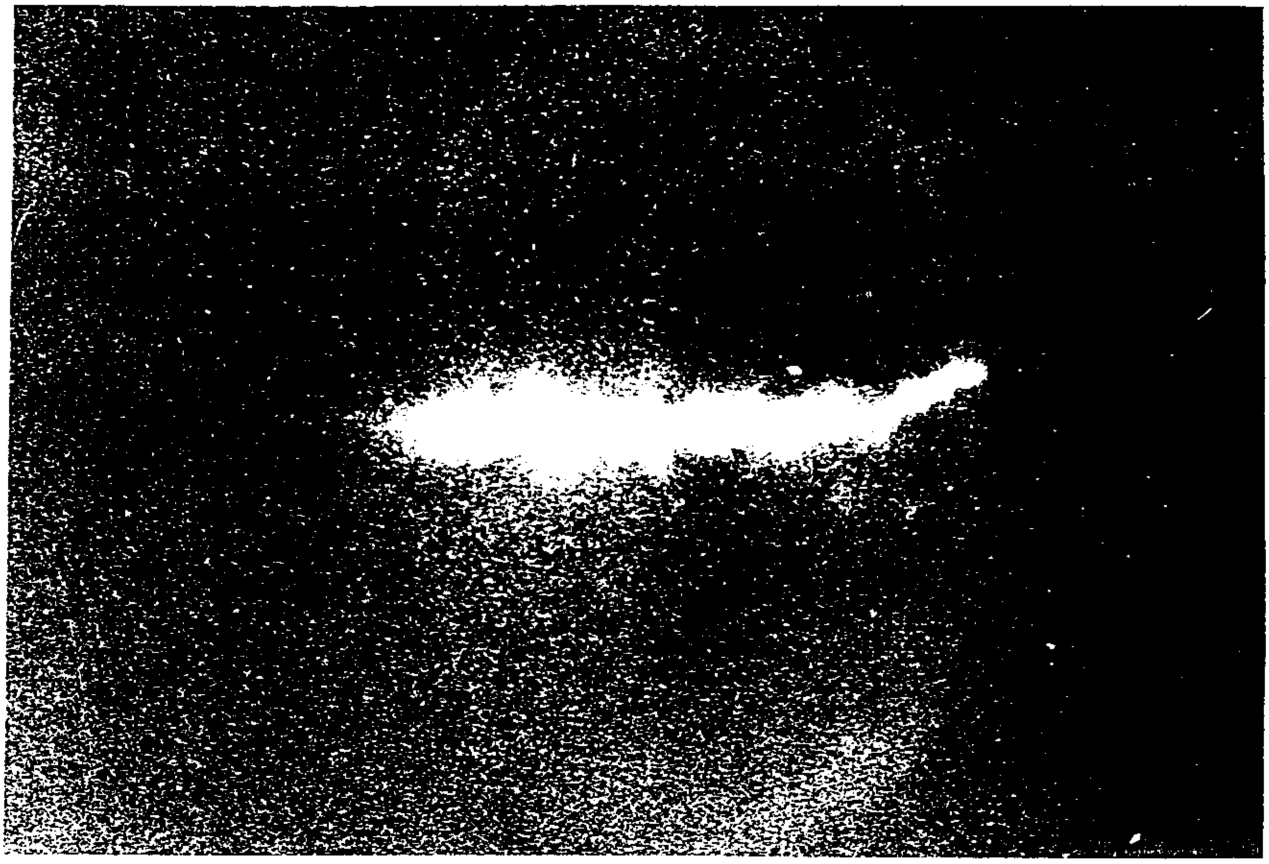

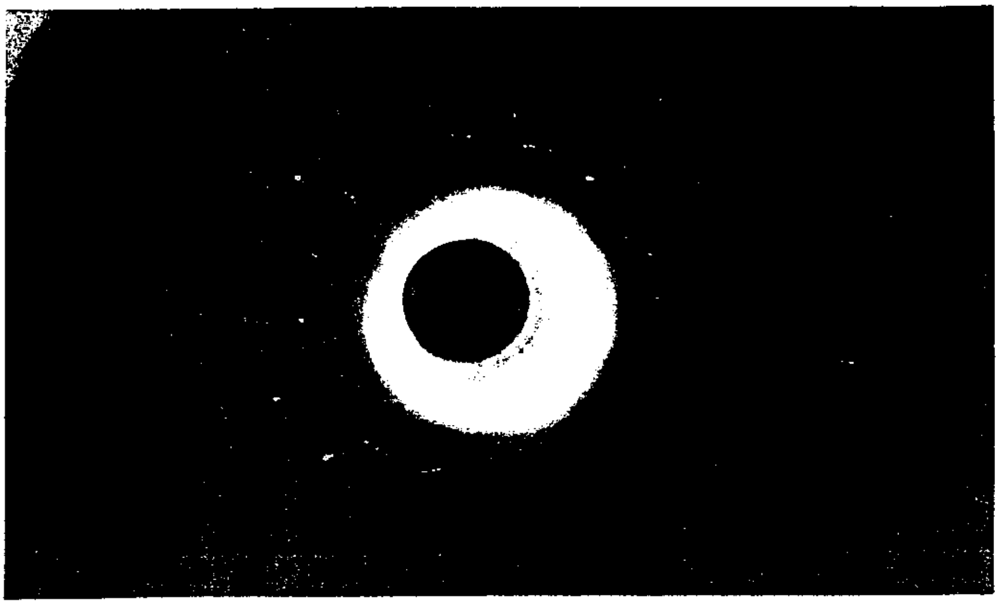

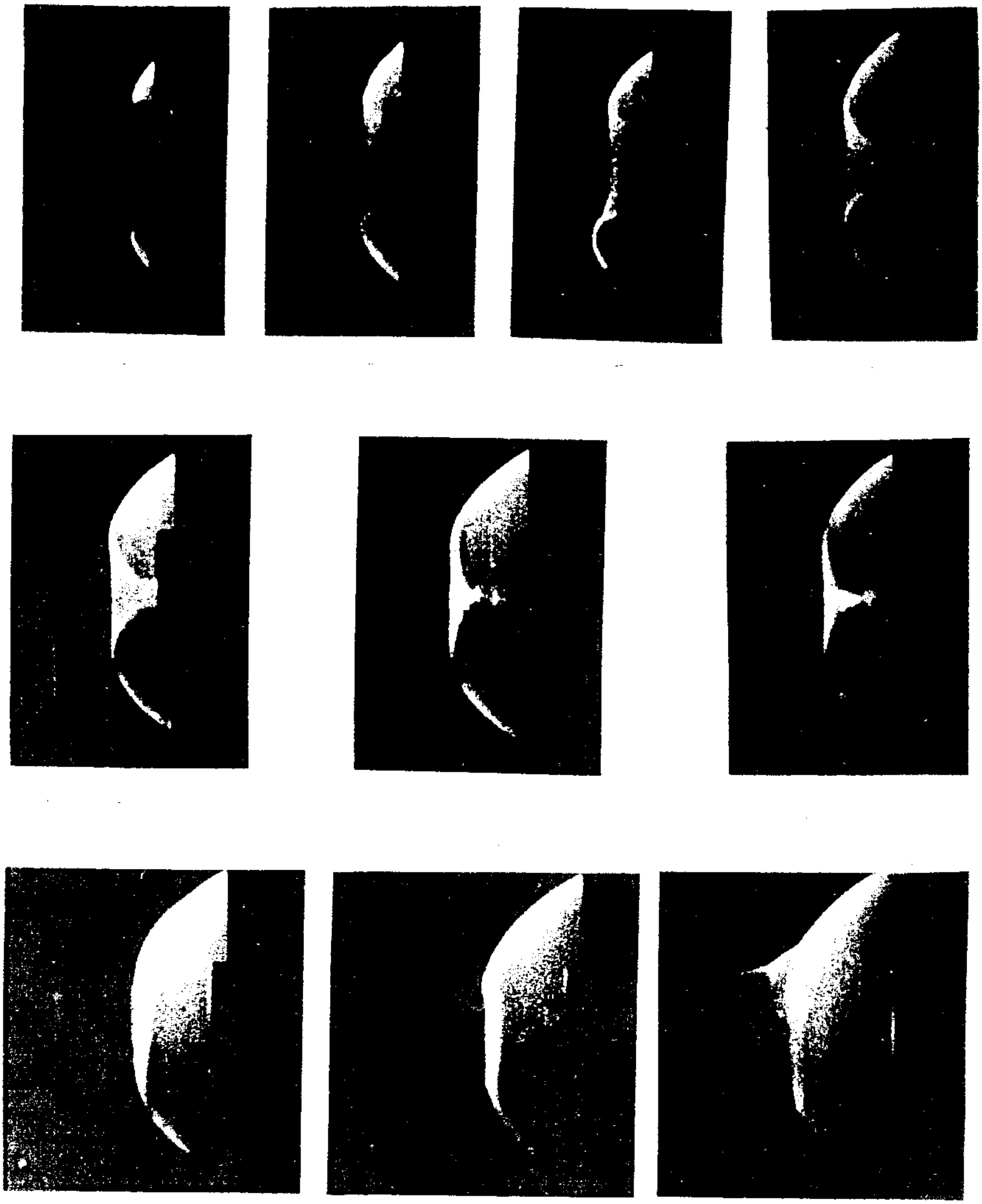

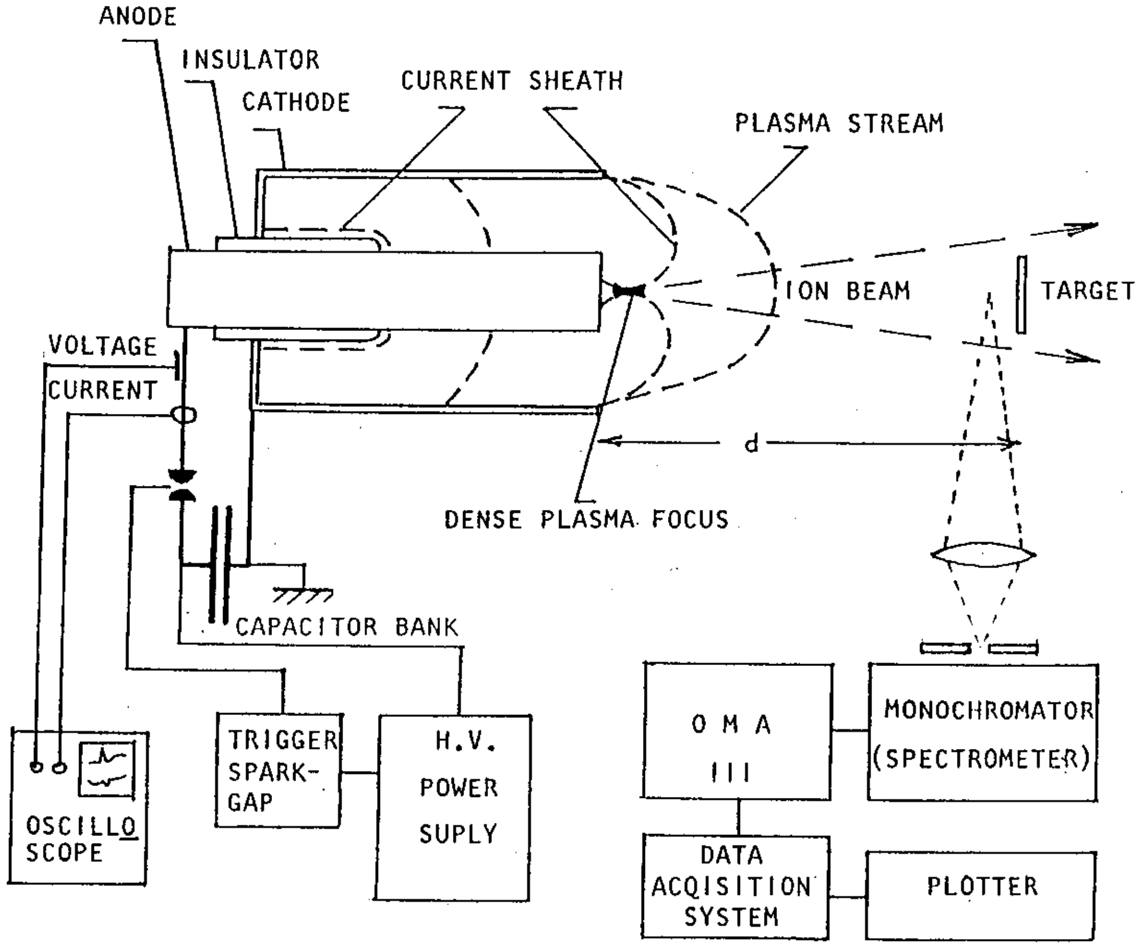

ANODE
INSULATOR
CATHODE
CURRENT SHEATH
PLASMA STREAM
ION BEAM
TARGET
VOLTAGE
CURRENT
d
DENSE PLASMA FOCUS
CAPACITOR BANK
TRIGGER SPARK-GAP
H.V. POWER SUPLY
OSCILLO SCOPE
O M A III
MONOCHROMATOR (SPECTROMETER)
DATA ACQISITION SYSTEM
PLOTTER

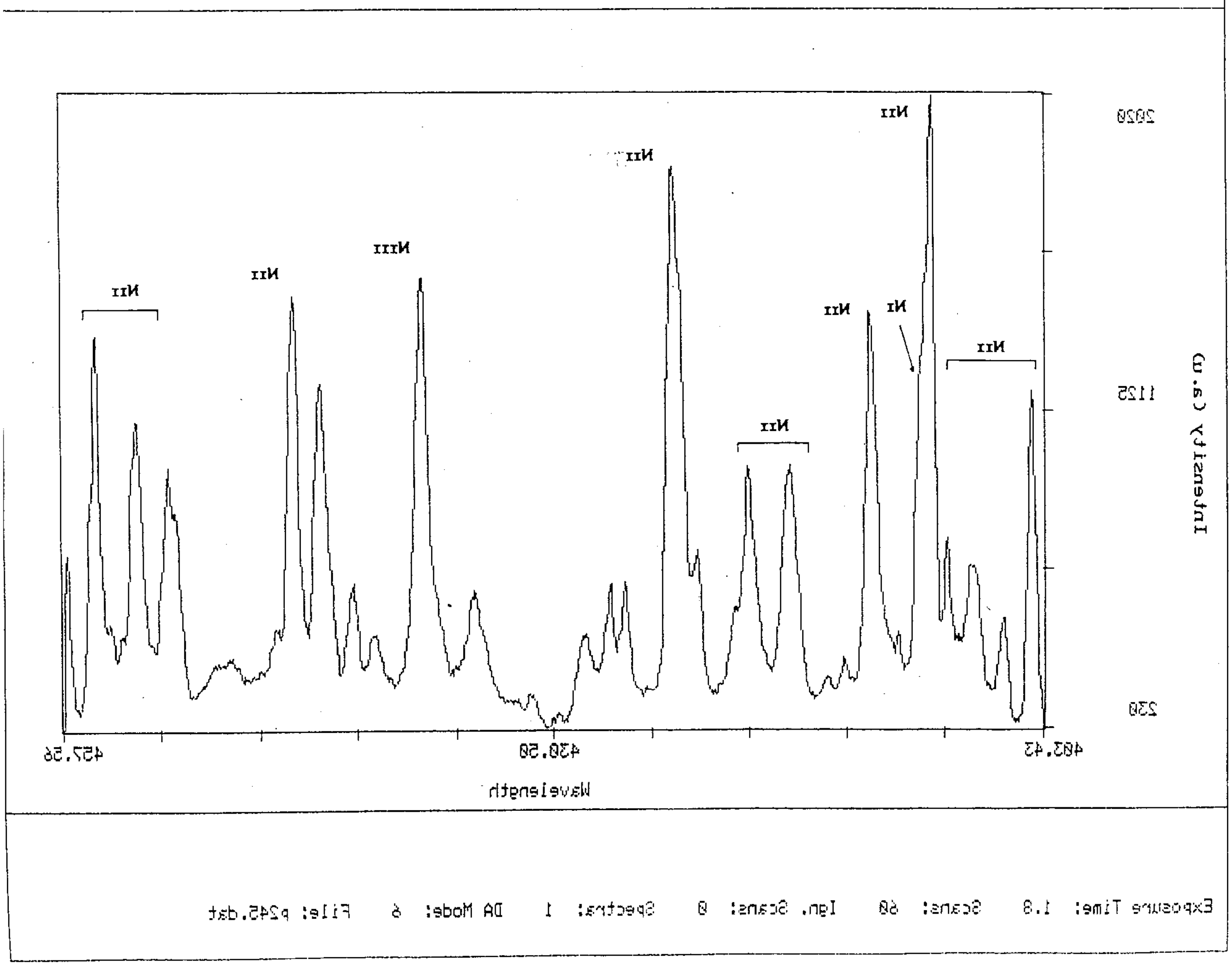

Intensity (a.u)
2020
1125
230
457.56
430.50
403.43
Wavelength
NII
NII
NIII
NII
NII
NII
NI
NII
NII
Exposure Time: 1.8 Scans: 60 Ign. Scans: 0 Spectra: 1 DA Mode: 6 File: p245.dat

PLASMA GUN: CHARACTERISTICS

GEOMETRY:

Anode:	$\Phi = 17mm$;	$l = 70mm$
Cathode:	$\Phi = 50mm$;	$l = 70mm$
Insulator:	$\Phi = 21mm$;	$l = 25mm$

PHYSICAL PARAMETERS:

Capacitor Bank: $C = 4\mu f$
$V = 25kV$
$L = 0.01\mu Hy$

Operating Pressure: 0.35 Torr.

ION BEAM: CHARACTERISTICS

Fluence per shot: $f < 4 \times 10^{14}\ cm^{-2}$

Pulse time duration: $\delta t > 200\ ns$

Ion beam energy (continuous spectral law): $N \sim E^{-2.4}$

N number of ions with E energy, and $E > 20keV$ per ion.

Higher (F) fluences can be obtained by accumulation of n single shots.

PENETRACION DE IONES ENERGETICOS EN SOLIDOS - RANGE. (ρ)

ION PENETRATION IN SOLIDS - RANGE (ρ)

$$E = \frac{1}{2} m_i v^2$$

$$\rho = f(E, Z)$$

(Z: Nº atomico)

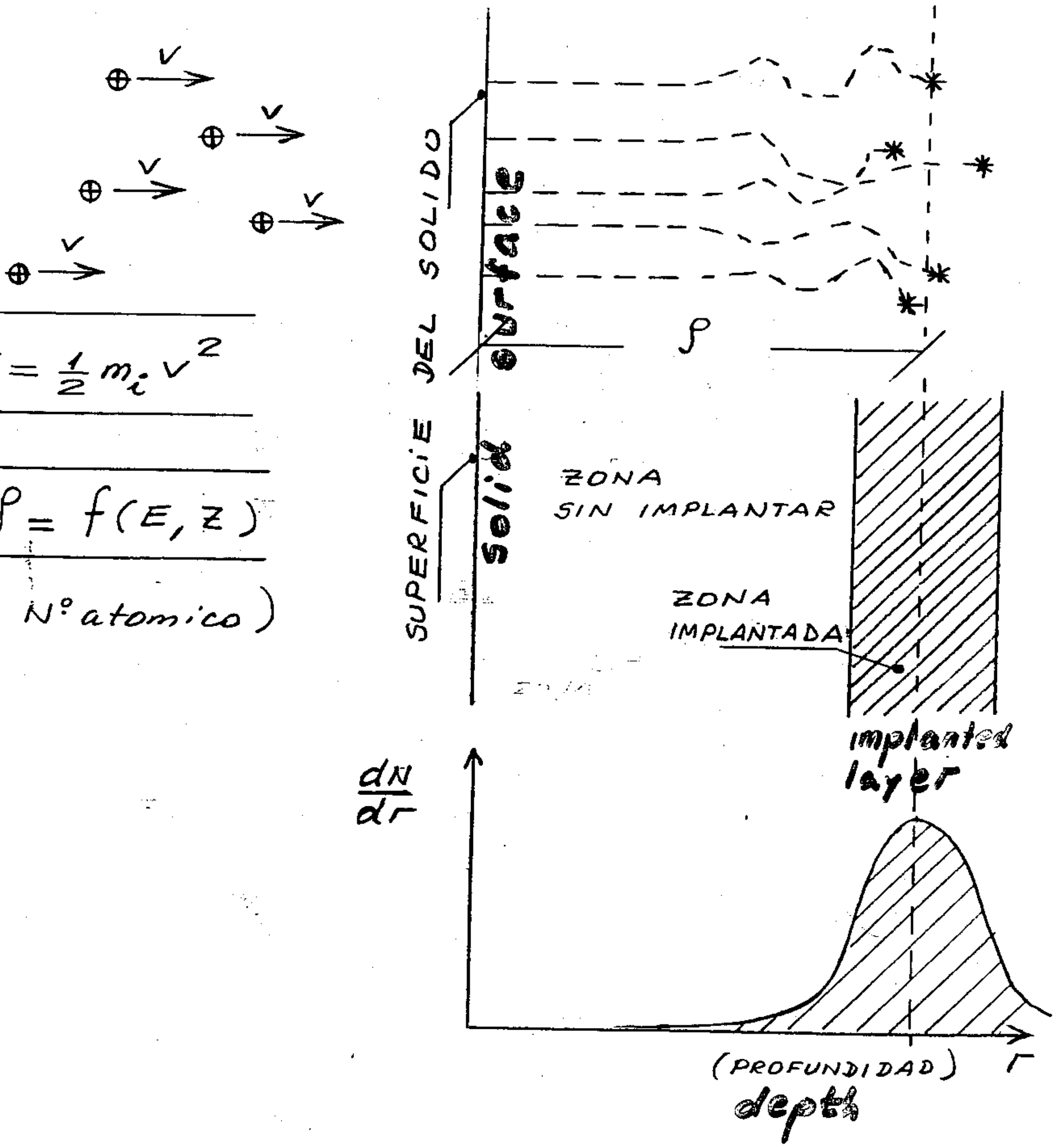

SURFACE TEMPERATURE EVOLUTION

The temperature evolution due to the interaction of pulsed nitrogen beams was studied using finite differences calculations.

Calculations were done assuming the following:

- **During penetration, the ions loose their kinetic energy gradually and uniformly**
- **Every ion stops at a depth equal to the RANGE corresponding to its kinetic energy E**
- **The ion energy is totally converted into thermal energy in the affected layer**
- **The only cause of cooling is the thermal conduction at the bulk of the sample**
- **The thermal constants of the implanted material (bulk) were used**
- **No boundary conditions were used**

The calculations were done for different ion beam pulses characteristics

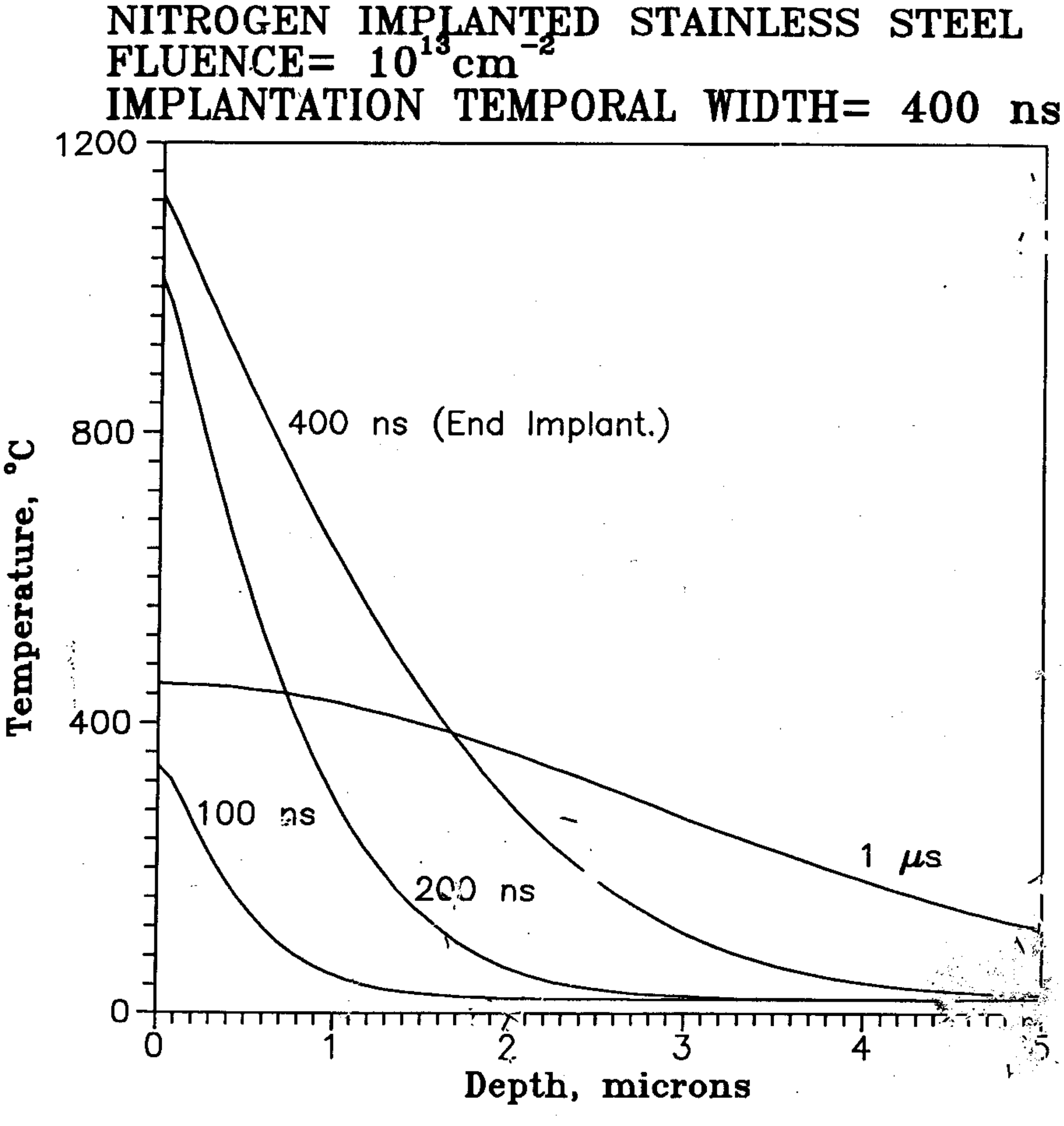
NITROGEN IMPLANTED STAINLESS STEEL
FLUENCE= 10^13 cm^-2
IMPLANTATION TEMPORAL WIDTH= 400 ns
1200
800
400
0
Temperature, °C
400 ns (End Implant.)
100 ns
200 ns
1 μs
0
1
2
3
4
5
Depth, microns

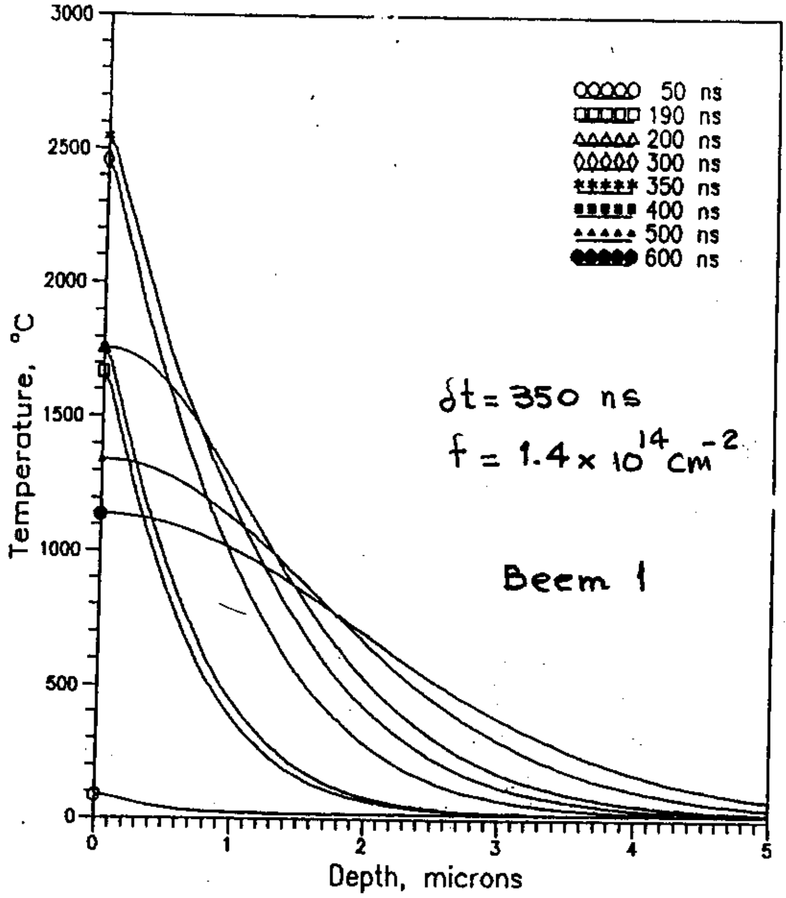

Temp. slope ~1500 K/μm

Heating speed ~15 K/ns

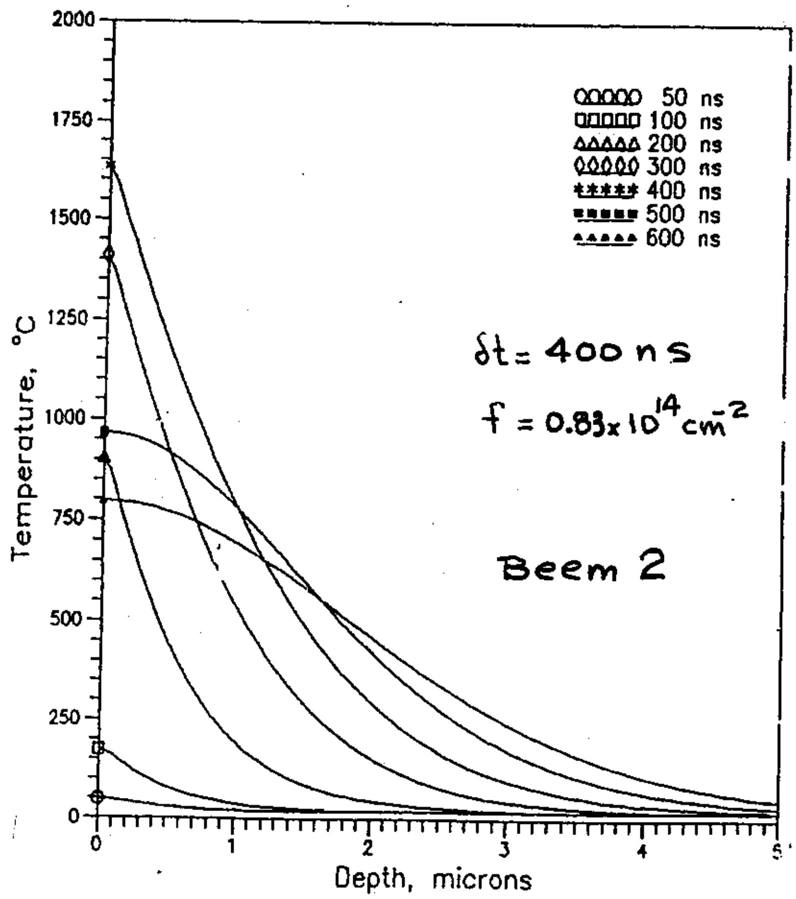

STAINLESS STEEL (AISI 304)

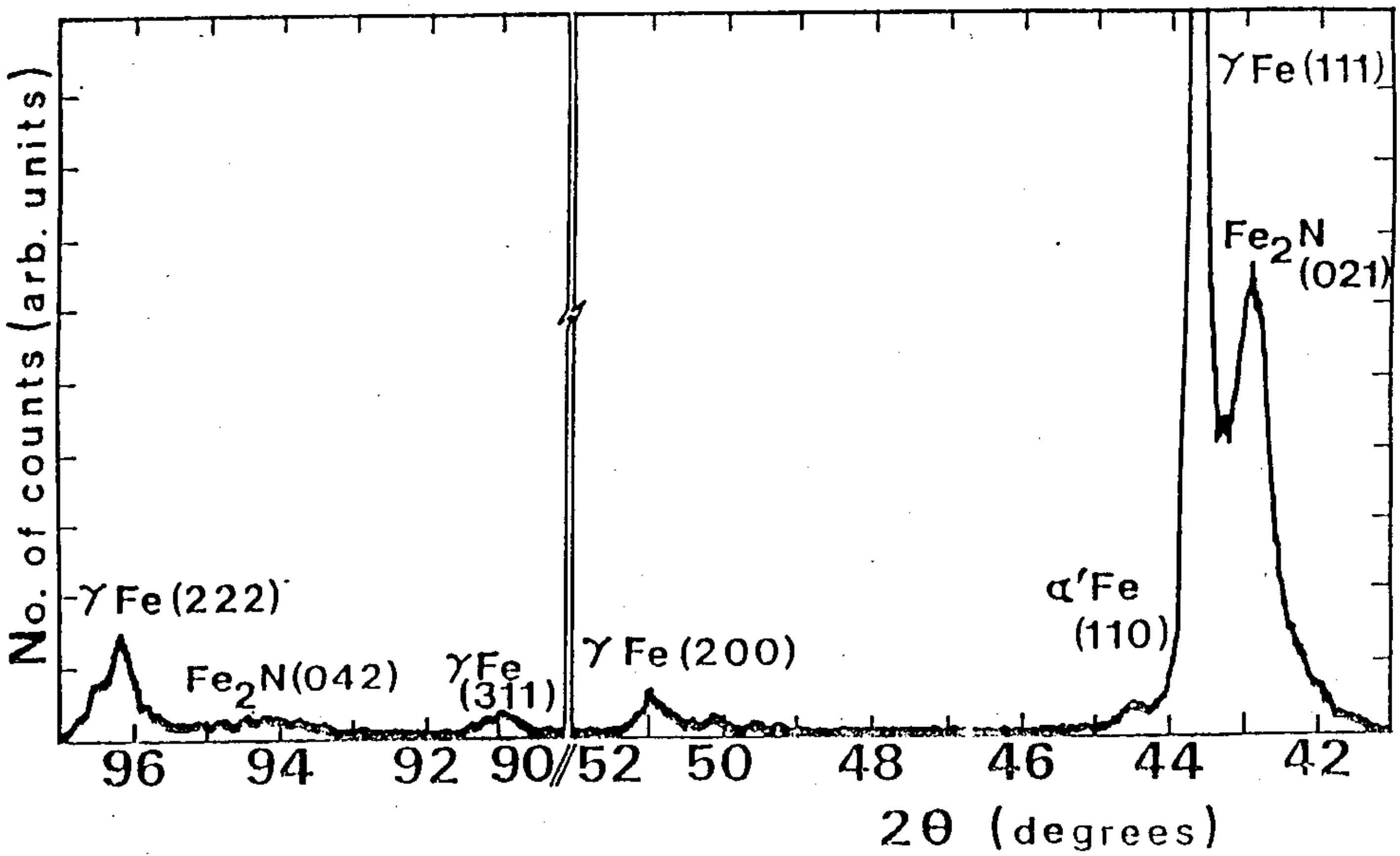

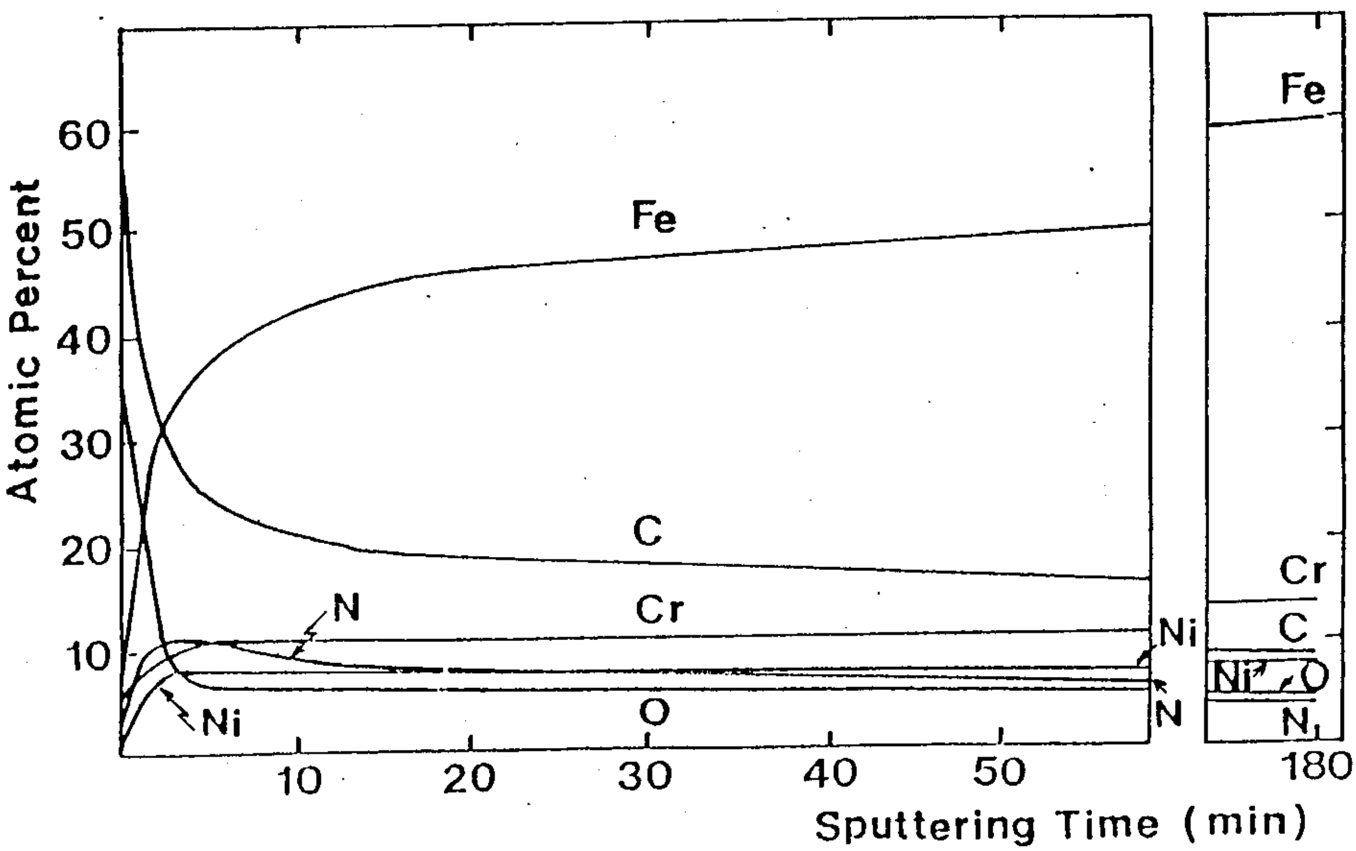

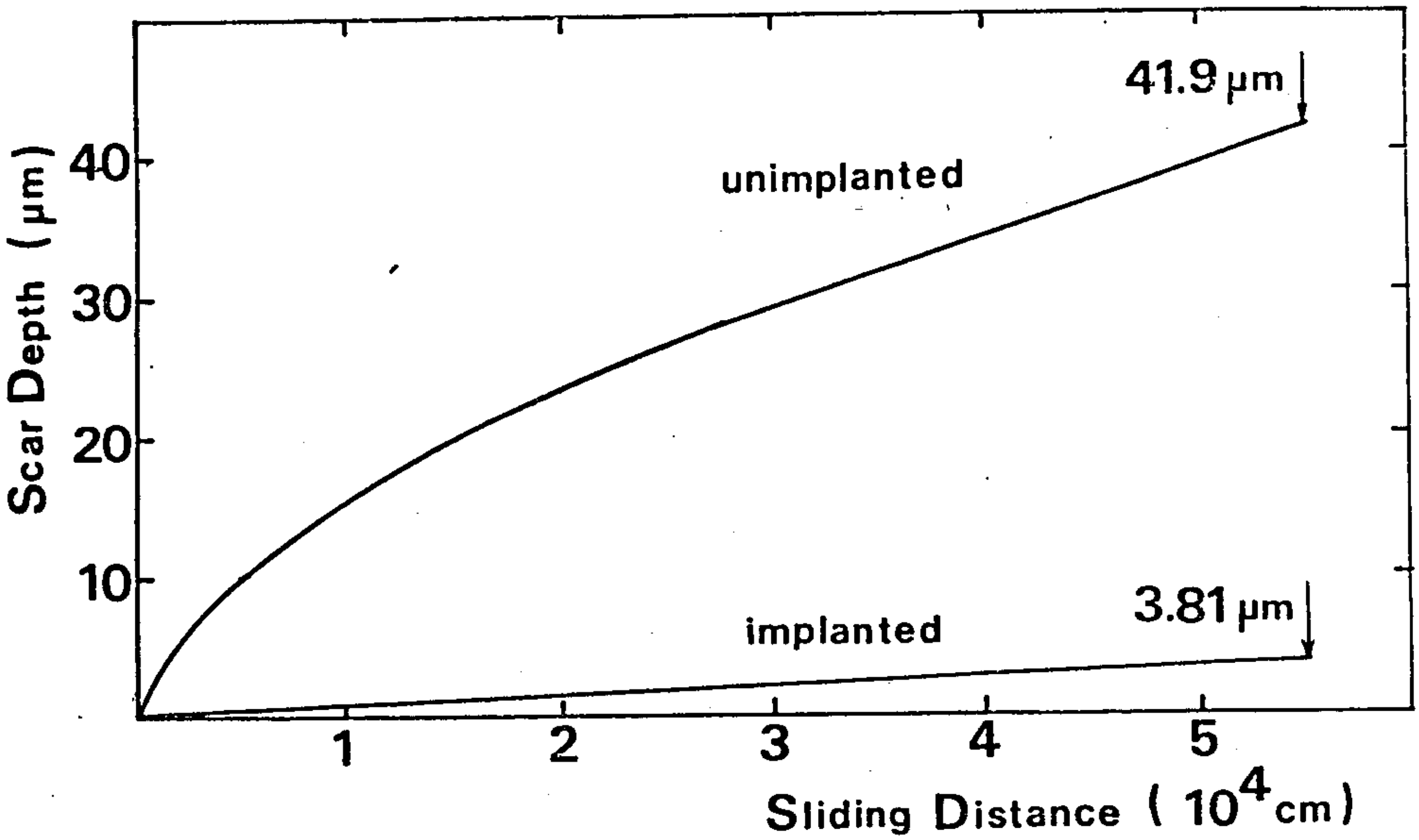
Scar Depth (μm)
40
30
20
10
unimplanted
41.9 μm
implanted
3.81 μm
1
2
3
4
5
Sliding Distance (10^4 cm)

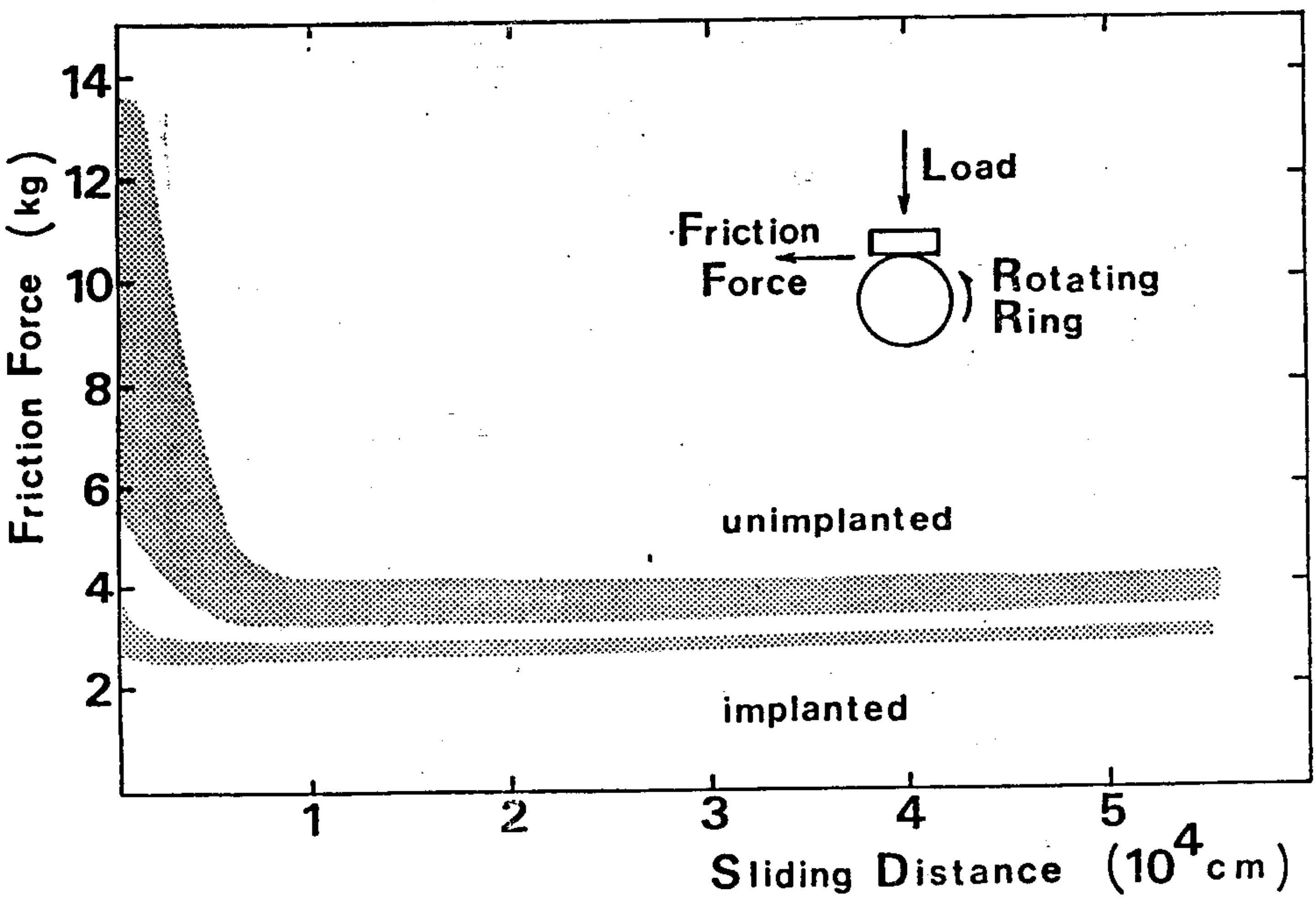
Friction Force (kg)
14
12
10
8
6
4
2
Load
Friction Force
Rotating Ring
unimplanted
implanted
1
2
3
4
5
Sliding Distance (10^4 cm)

HIGH SPEED (M2) STEEL

XPS

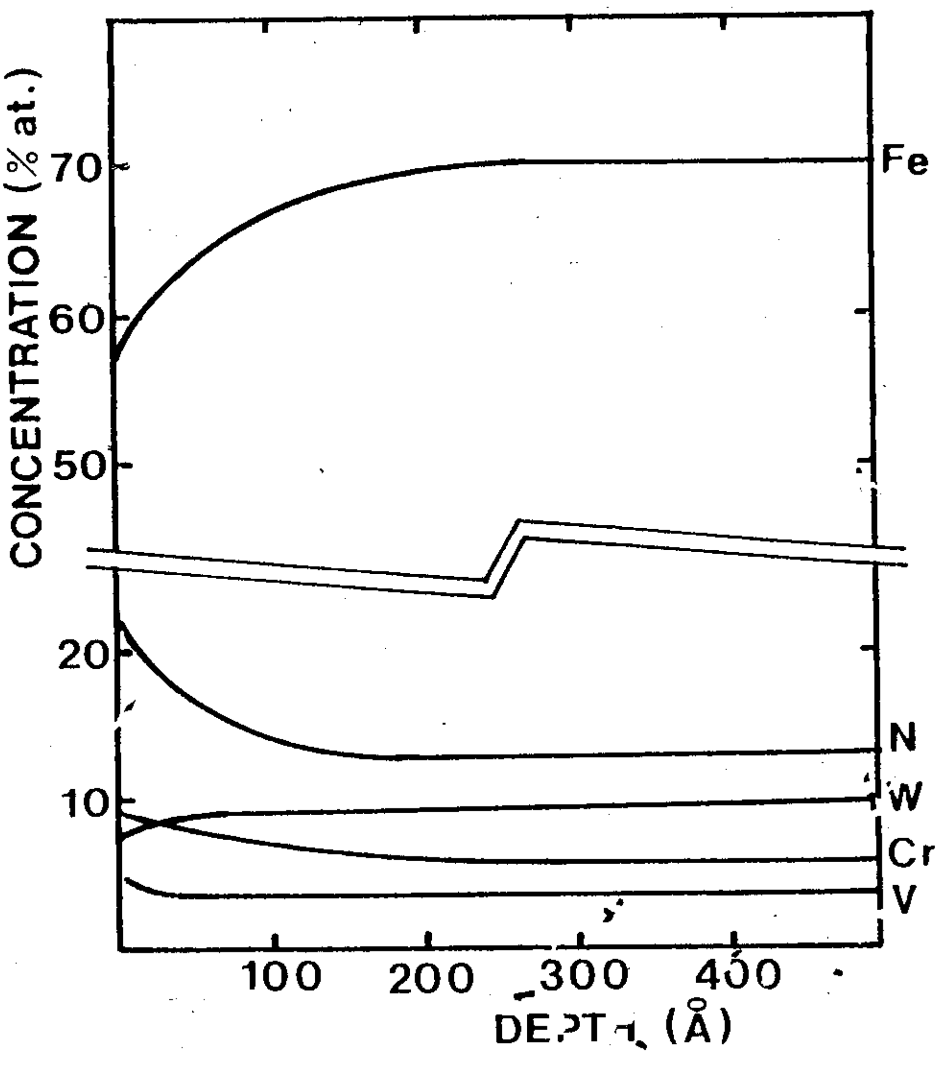

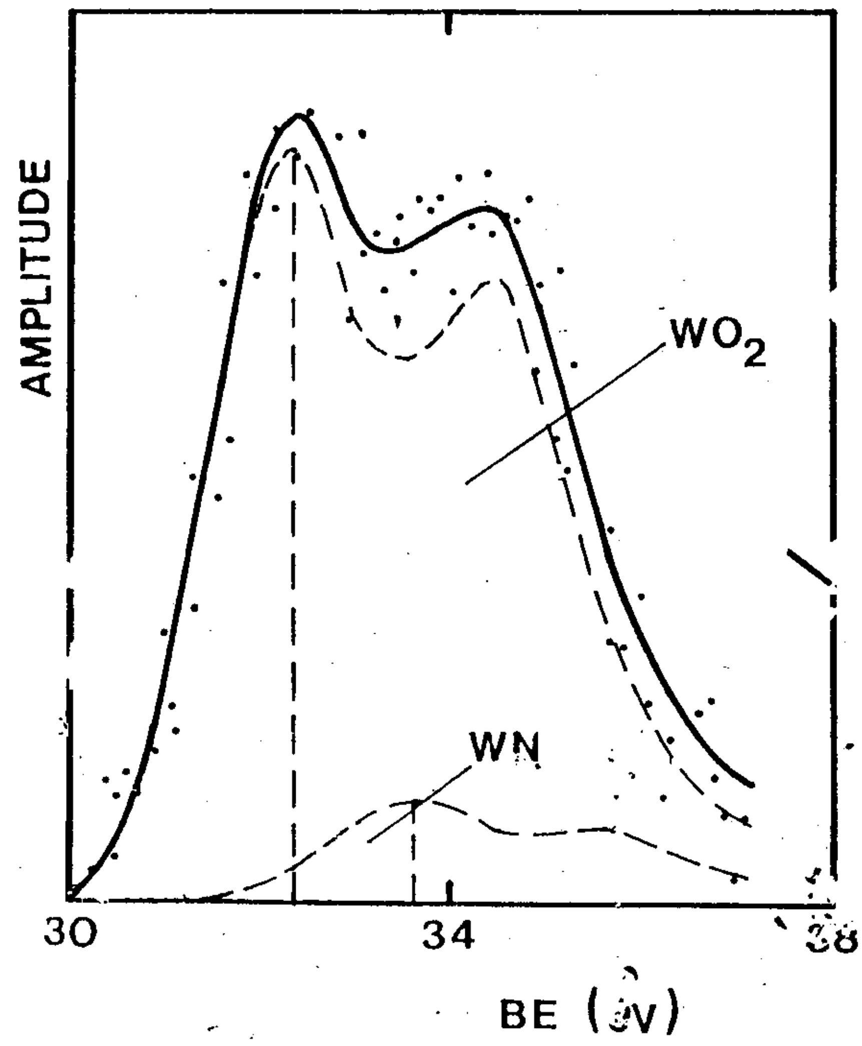
AMPLITUDE
WO2
WN
30
34
38
BE (eV)

Steel: 0.53% C , 3.8% Ni , 1,65% Cr

MICROHARDNESS VICKERS (25 gr.)

IMPLANTATION CONDITIONS		MICROHARDNESS
fluence [cm^{-2}]	Δt [ns]	HVN
non implanted	-------	270 ± 10
5×10^{15}	400	260 ± 10
5×10^{15}	350	270 ± 20
5×10^{15}	300	550 ± 70

(In collaboration with Dr. A.R. da Costa, Escola de Minas, Univ. Fed. Ouro Preto, Brasil).

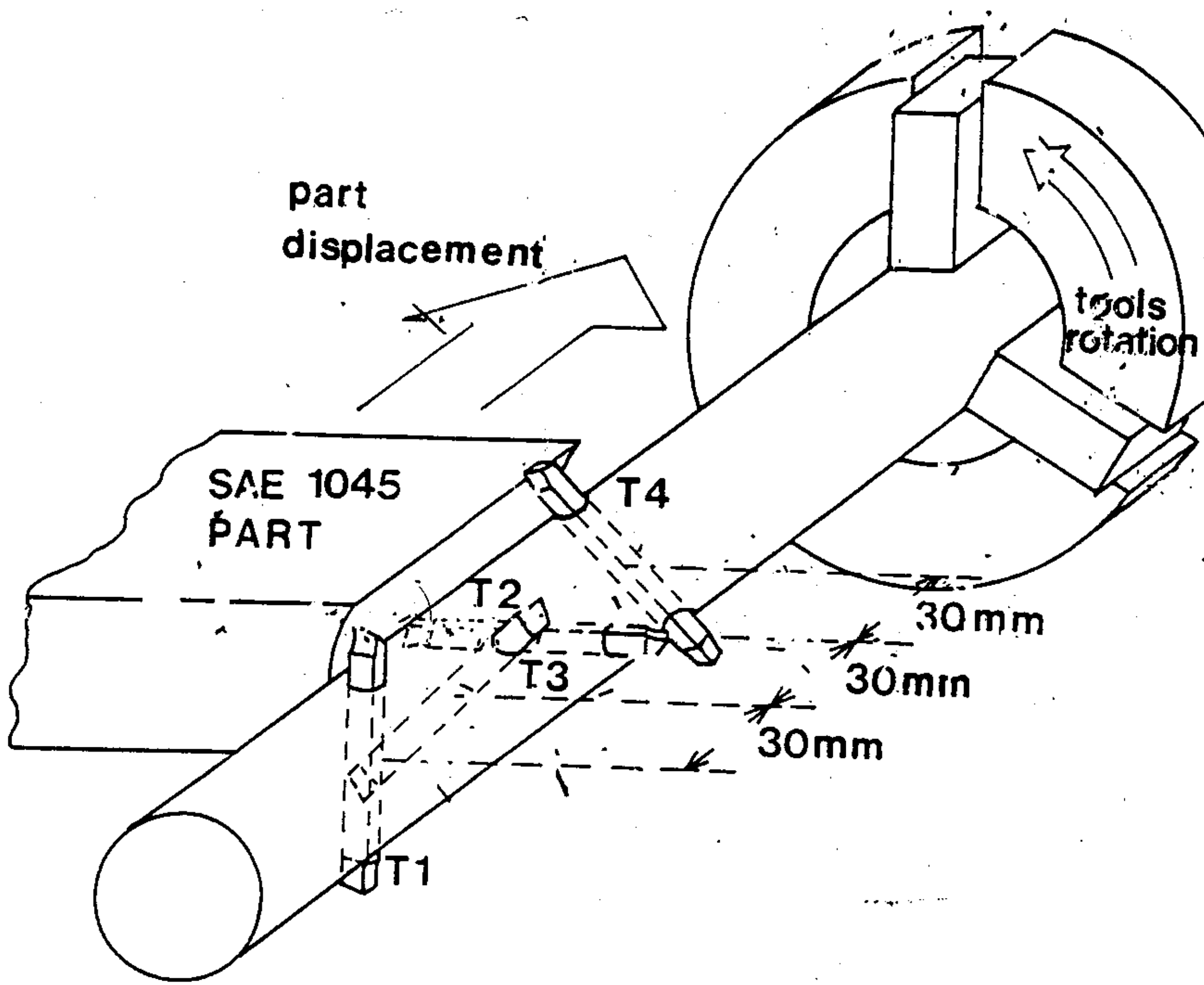
part
displacement
SAE 1045
PART
T1
T2
T3
T4
30mm
30mm
30mm
tools
rotation

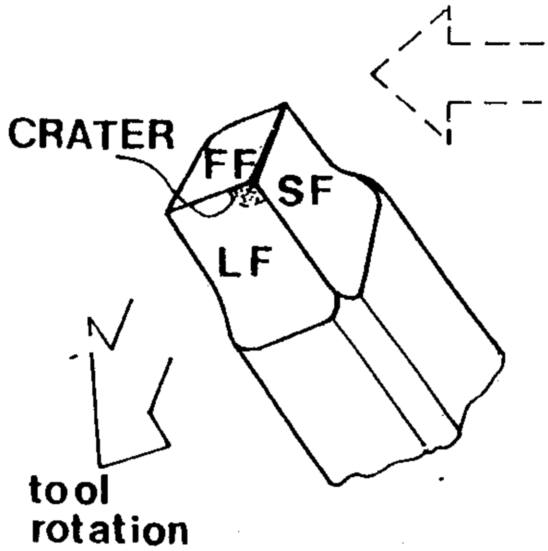
CRATER
FF
SF
LF
tool
rotation

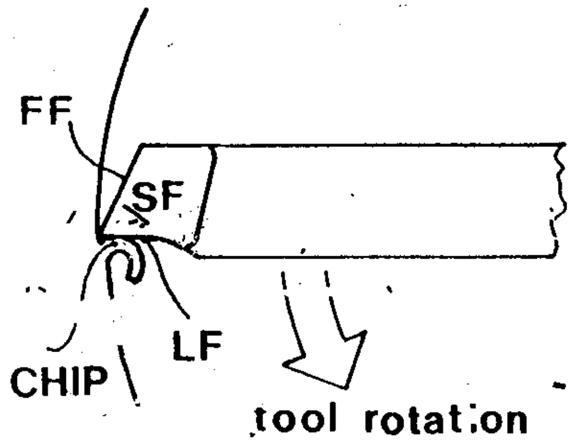
FF
SF
CHIP
LF
tool rotation

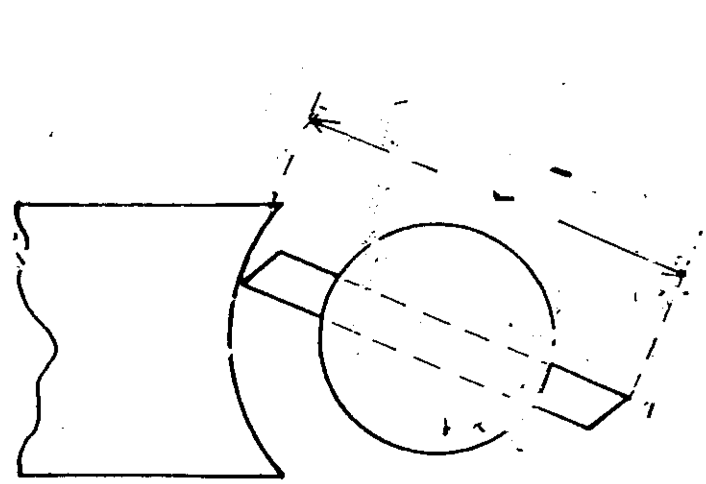

TiN_x (1.1 > x > 0.7)

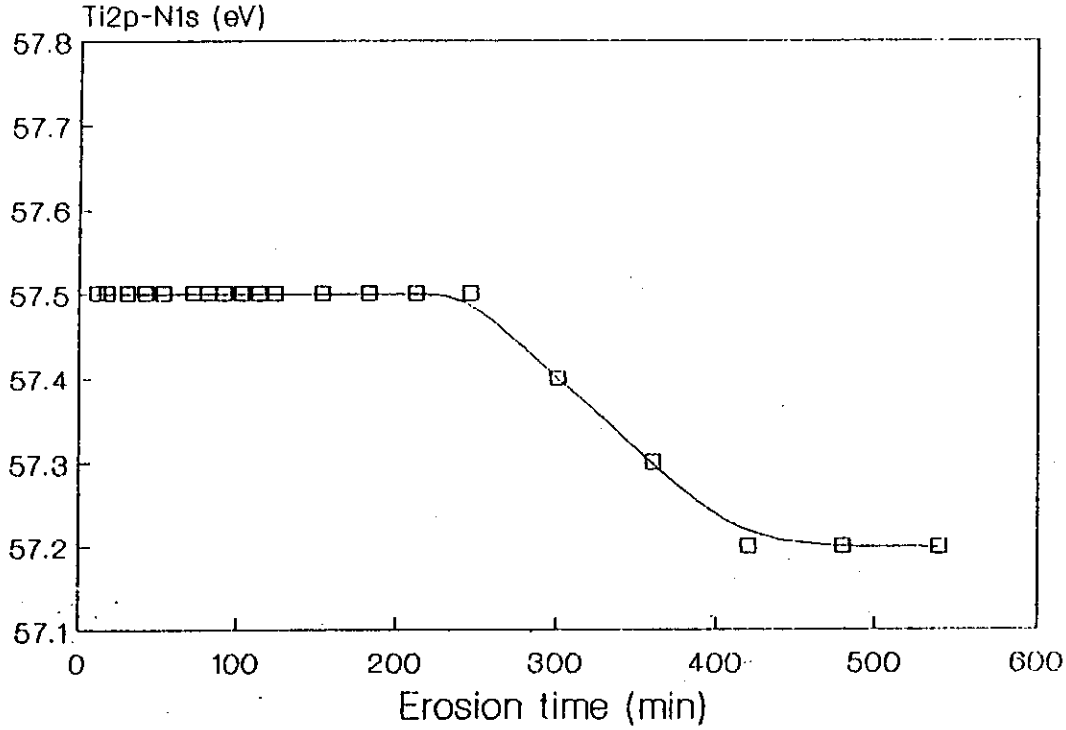

Ti2p-N1s (eV)
57.8
57.7
57.6
57.5
57.4
57.3
57.2
57.1
0
100
200
300
400
500
600
Erosion time (min)

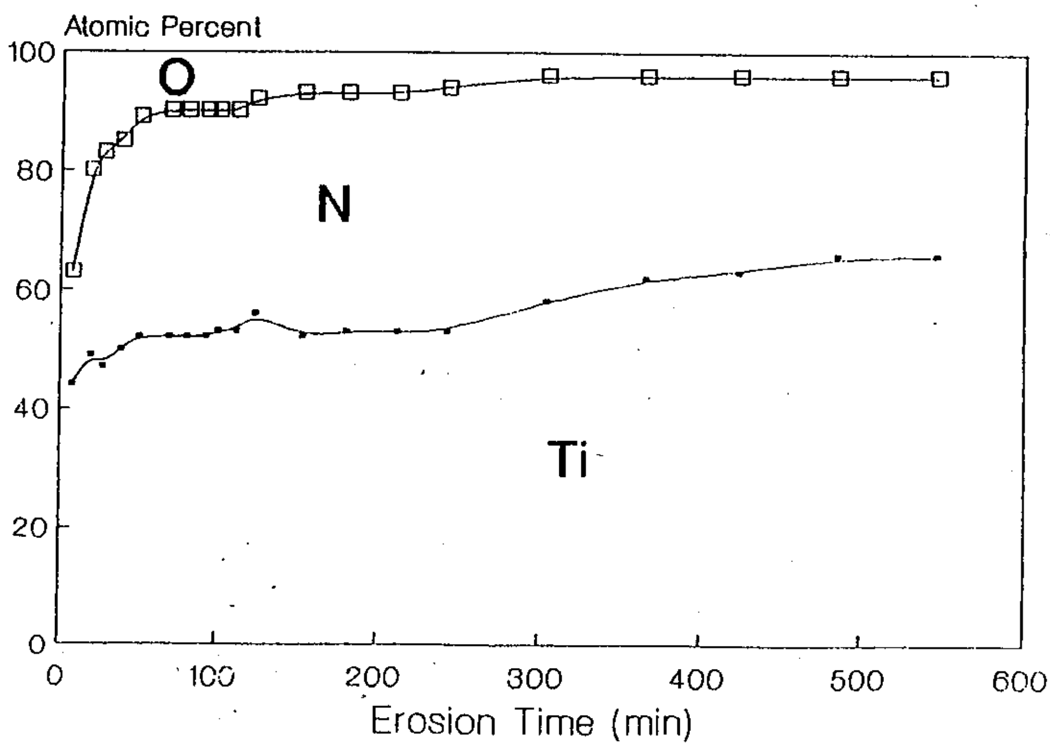

Atomic Percent
100
80
60
40
20
0
O
N
Ti
0
100
200
300
400
500
600
Erosion Time (min)

MICROHARDNESS

HV (Vickers microhardness)

Load: 5 g.

Penetration depth: ~ 0.6μm.

RESULTS:

Pure Titanium: HV = 270 kg/mm^2

Implanted in conditions
A and **B**: HV = 655kg/mm^2

RESIDUAL STRESSES

X-Ray diffraction techniques

{211} peaks, Cr K_α radiation

TABLE 1
Surface residual stress evolution with Nitrogen ions implantation in the AISI 1075 ferritic steel.

Sample	Rolling Dir.	Transv. Dir.
non-implanted	232±40 MPa	245±15 MPa
1.5 10^{16} Ions.cm-2	-286±24 MPa	-----
1.5 10^{17} Ions.cm-2	-261±50 MPa	-280±37 MPa

TABLE II
Surface Residual stresses in the M2 Steel implanted with Nitrogen Ions.

Sample	Rolling Dir.	Transv. Dir.
non-implanted	-880±67 MPa	-768±35 MPa
1.5 10^{16} Ions.cm-2	-304±25 MPa	-358±52 MPa
2.5 10^{16} Ions.cm-2	342±51 Mpa	454±87 MPa

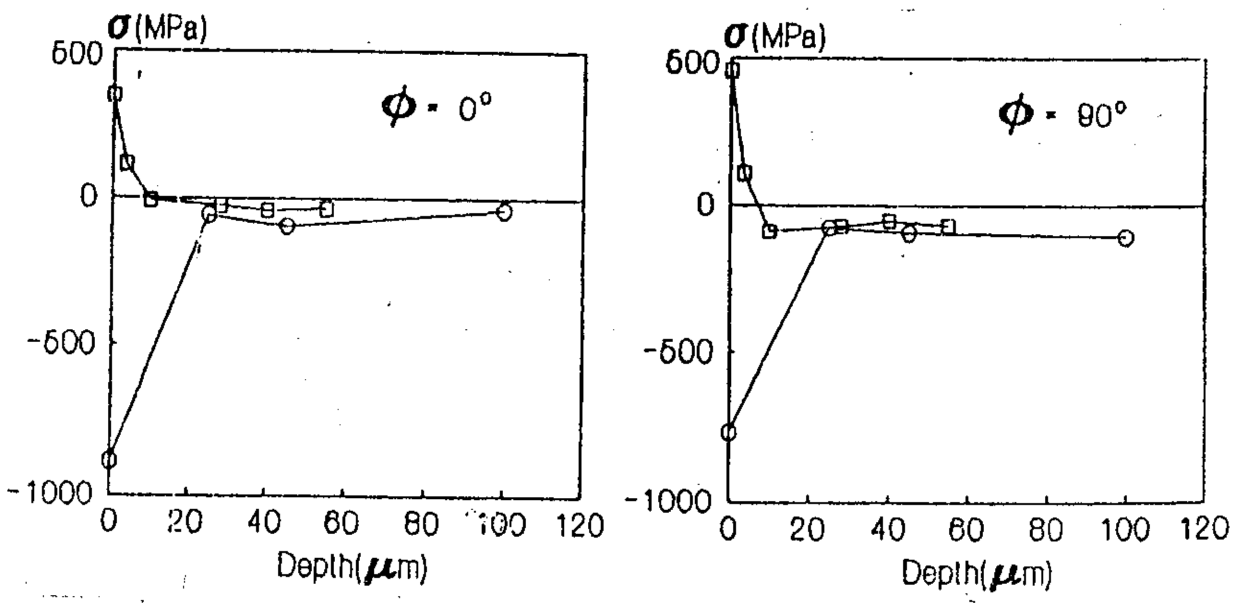

: Residual Stress evolution with depth in M2 steel.
□ Nitrogen implantation dose: 3.5 10^{18} Ions cm^{-2}.

6.5 Evaluación de deformaciones y tensiones residuales

Medición de tensiones residuales (relajación mediante calentamiento local).

Determinación de deformaciones residuales generadas por implantación iónica.

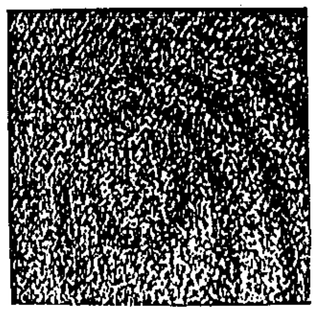

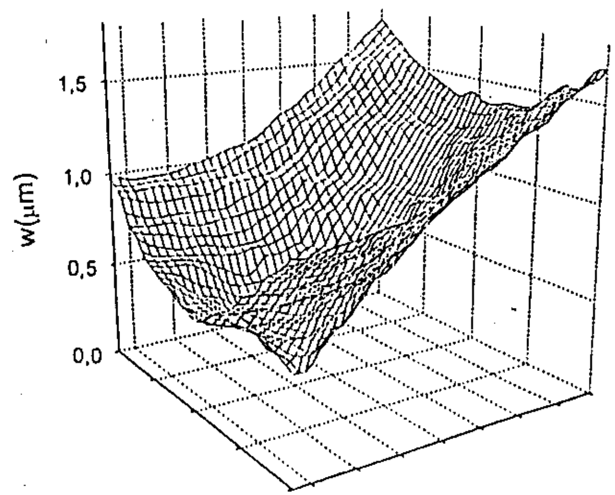

7. Conclusiones

Se espera que el desarrollo de nuevos tipos de lasers compactos y componentes electro-ópticas permitirá en los próximos años la aplicación de la técnica de DSPI a la solución de distintos problemas industriales.

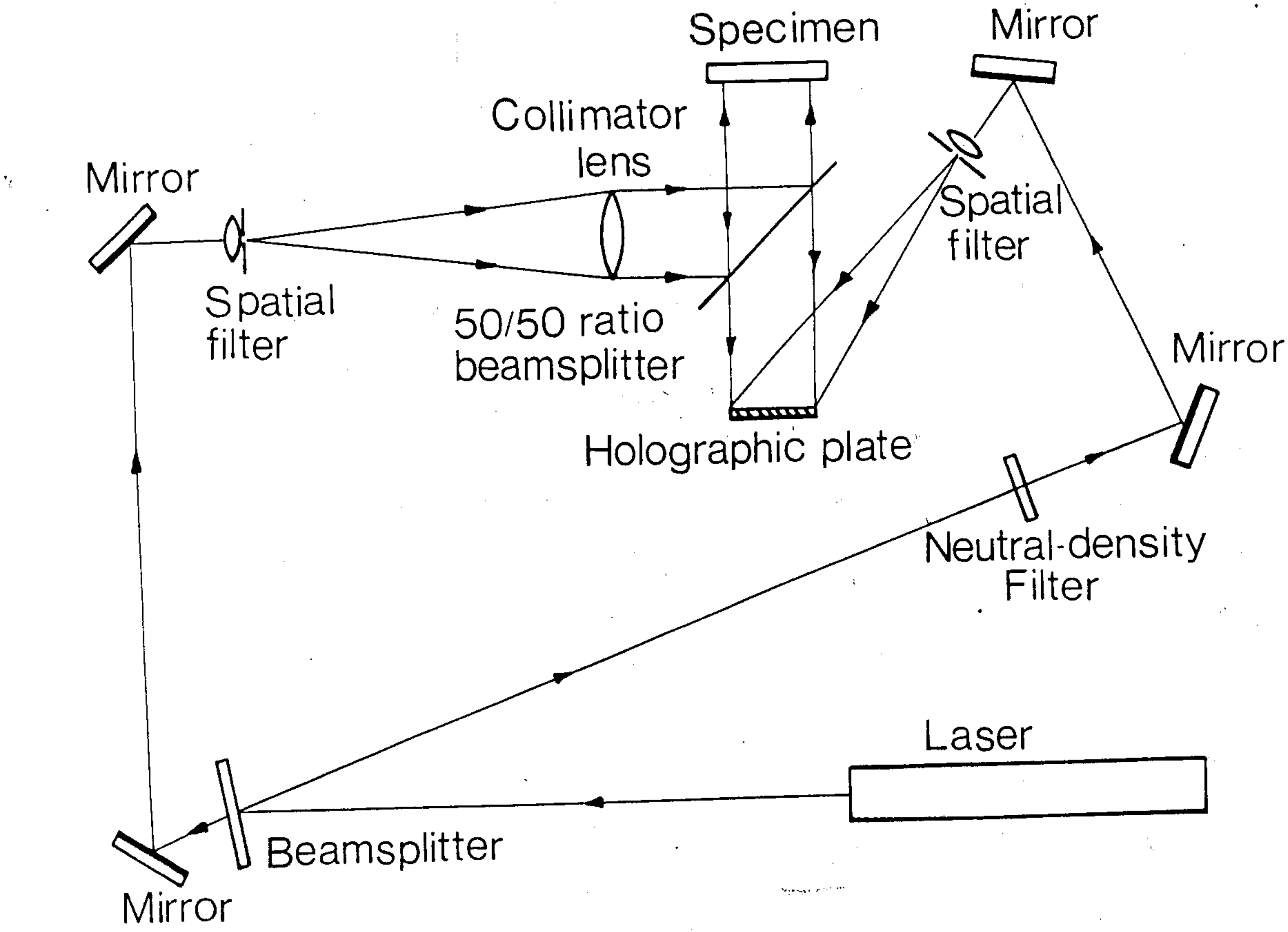
Specimen
Mirror
Collimator
lens
Mirror
Spatial
filter
Spatial
filter
50/50 ratio
beamsplitter
Mirror
Holographic plate
Neutral-density
Filter
Laser
Beamsplitter
Mirror

CONCLUSIONS

- **Plasma Focus is an efficient plasma accelerator**
- **High energy, ultra short time duration pulsed plasmas can be generated several times per second**
- **Low cost (($100.000), portable (1 meter, 30kg) accelerator can be constructed**
- **Surface modification of steels and other alloys are induced, with important tribological and mechanical properties improvement**
- **These changes can be mainly attributed to the thermal effect (thermal shock), in addition to other effects like ion implantation when, for example nitrogen is used as the carrier gas in the discharge**

En la Figura 3 se puede ver el sistema completo, incluyendo la cámara de descarga (**CD**), y en la Figura 4 una fotografía con el módulo terminado.

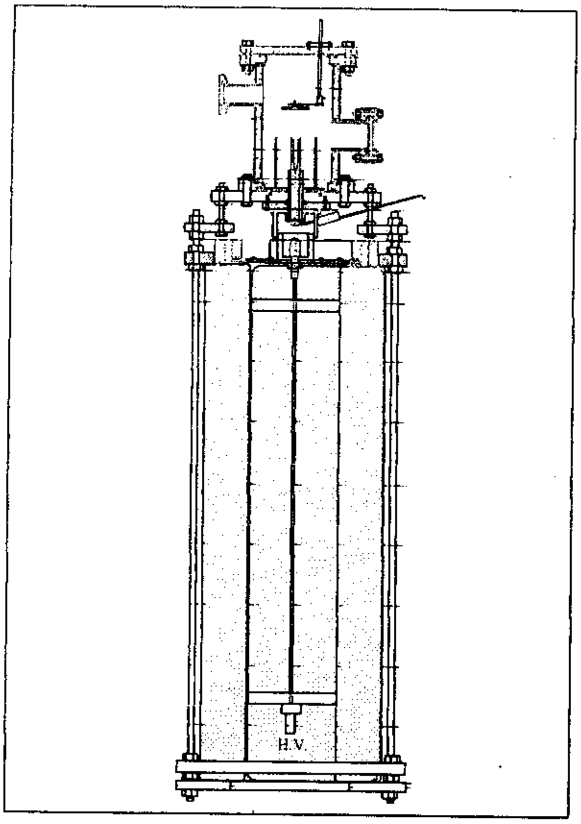

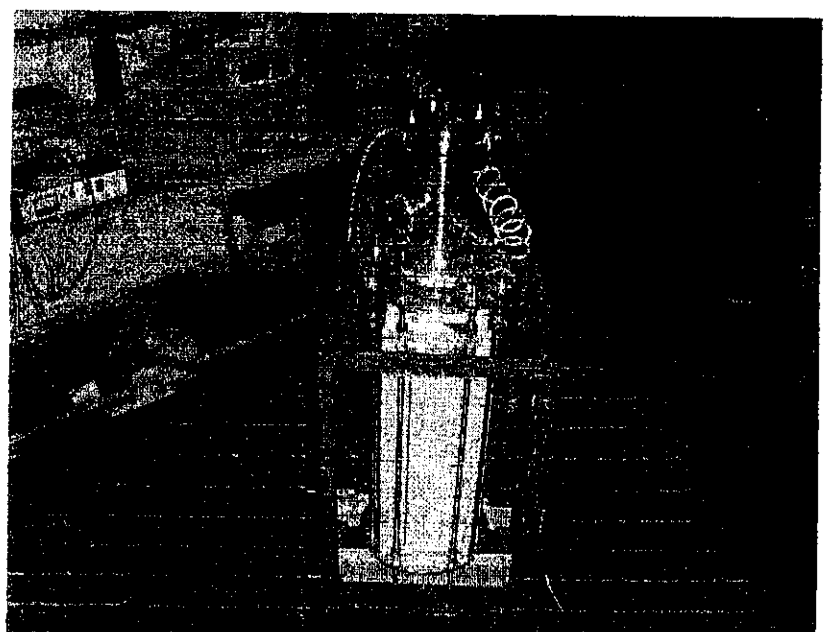

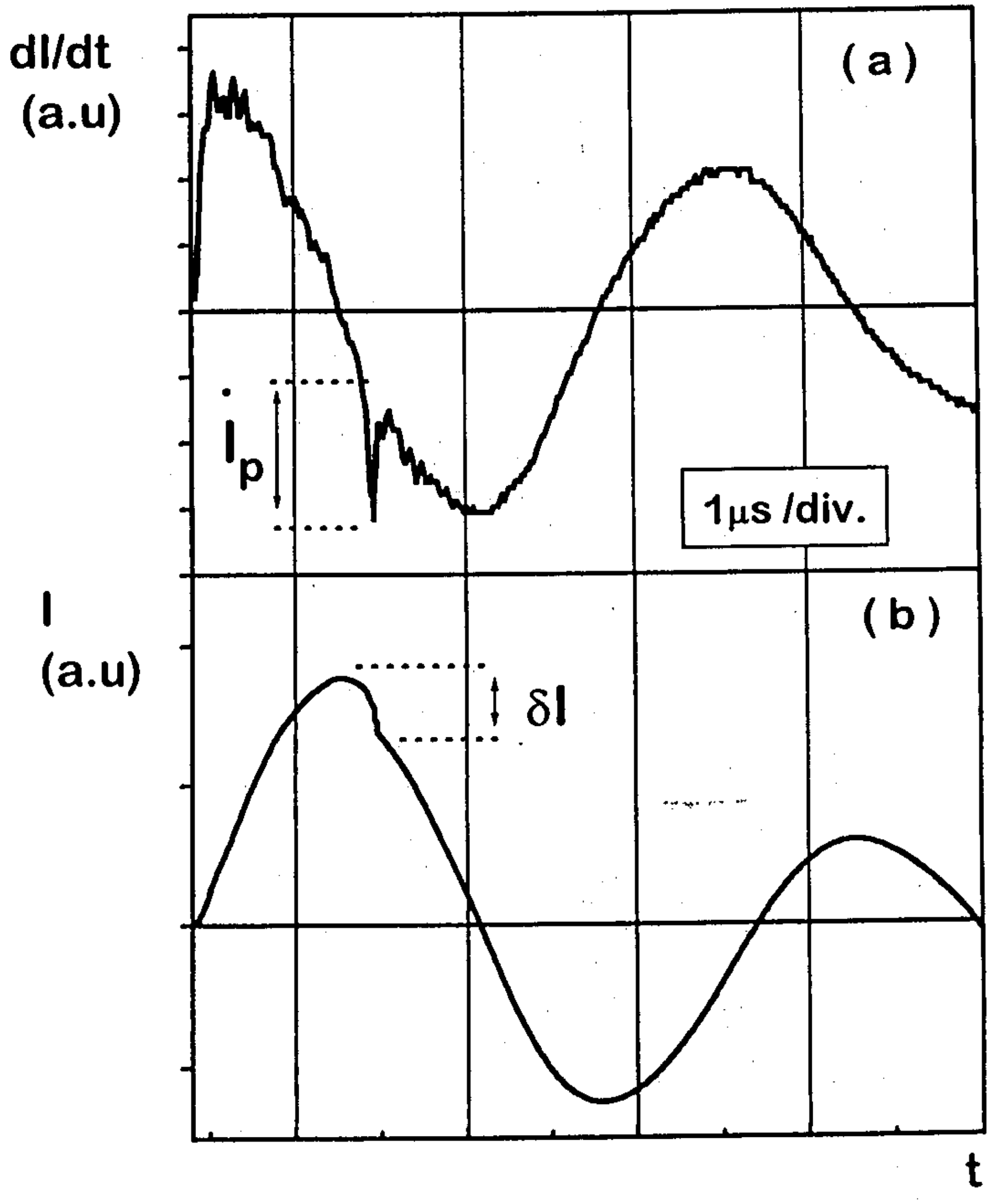
dI/dt
(a.u)
(a)
$\dot{I}_p$
1μs /div.
I
(a.u)
(b)
δI
t

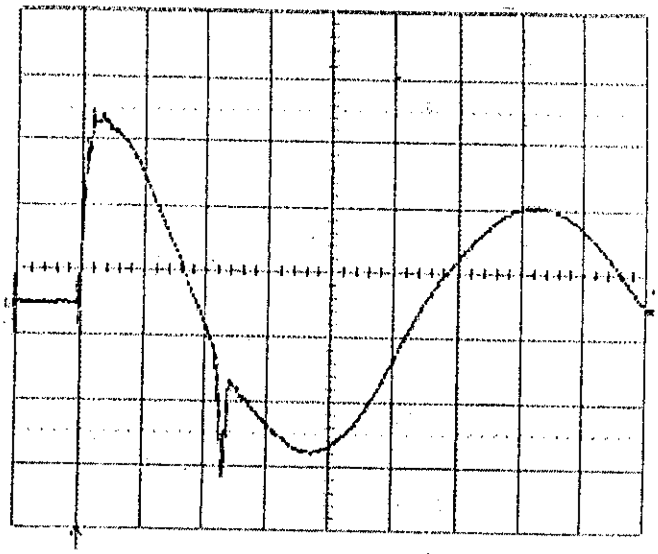

V = 17.4 kV

p = 230 mbar

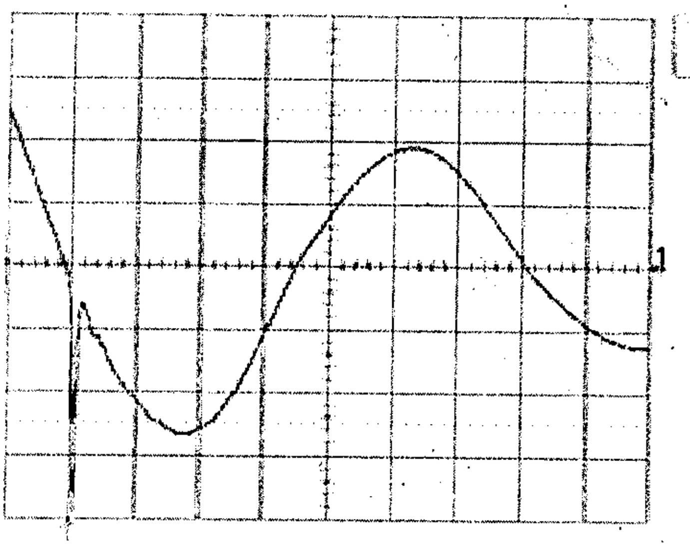

V = 20.0 kV

p = 230 mbar

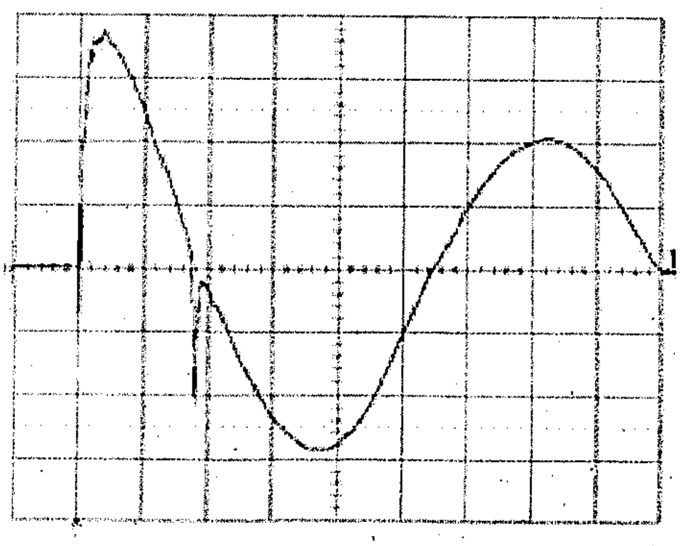

V = 23.2 kV

p = 230 mbar

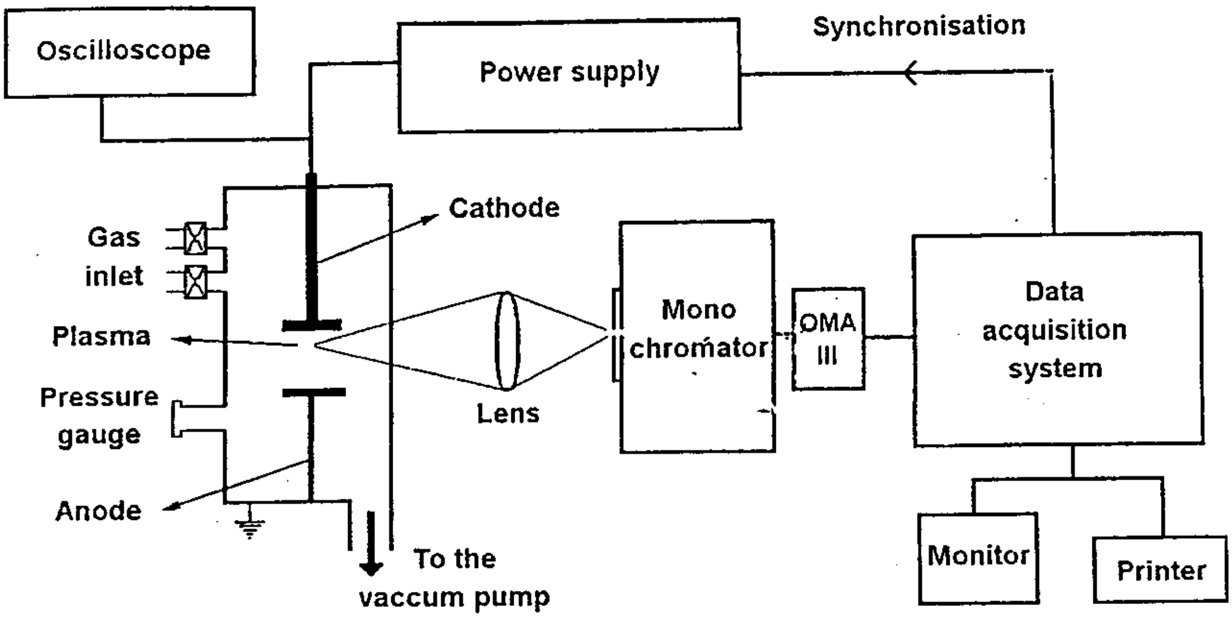
Oscilloscope
Power supply
Synchronisation
Cathode
Gas
inlet
Plasma
Pressure
gauge
Anode
Lens
Mono
chromator
OMA
III
Data
acquisition
system
Monitor
Printer
To the
vaccum pump

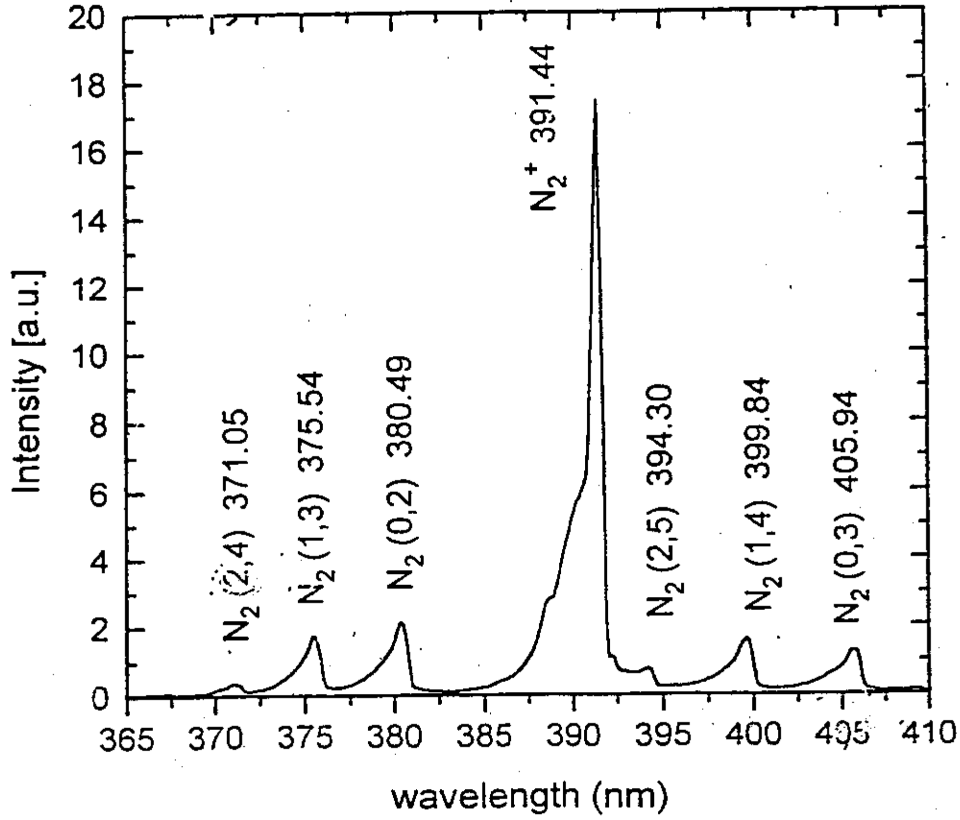
Intensity [a.u.]
wavelength (nm)
N2 (2,4) 371.05
N2 (1,3) 375.54
N2 (0,2) 380.49
N2+ 391.44
N2 (2,5) 394.30
N2 (1,4) 399.84
N2 (0,3) 405.94
0
2
4
6
8
10
12
14
16
18
20
365
370
375
380
385
390
395
400
405
410

REACTOR CHAMBER DURING AN ION NITRIDING PROCESS

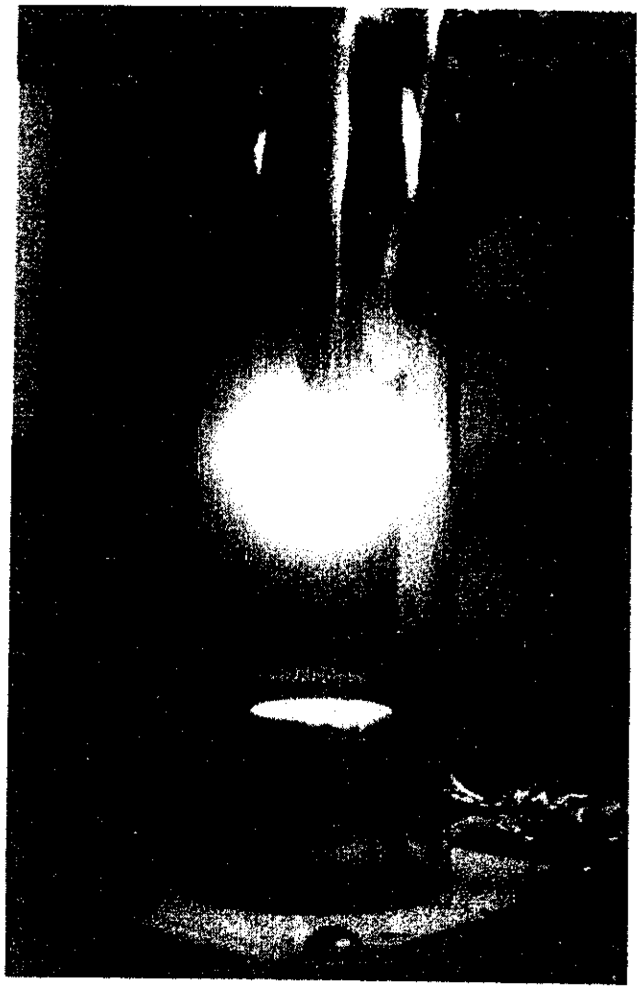

NEGATIVE GLOW AROUND THE CATHODE

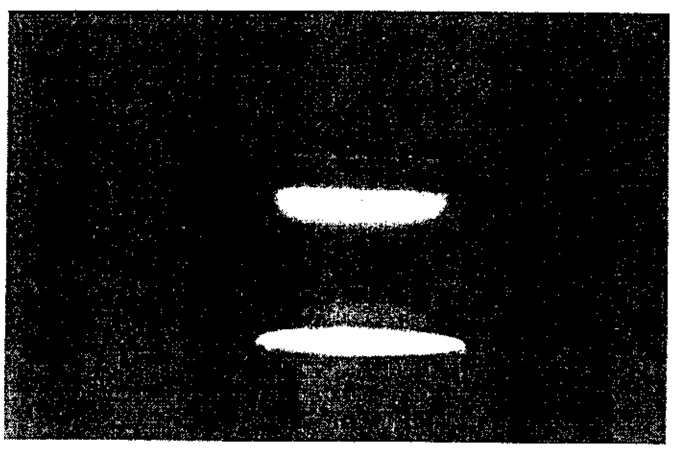

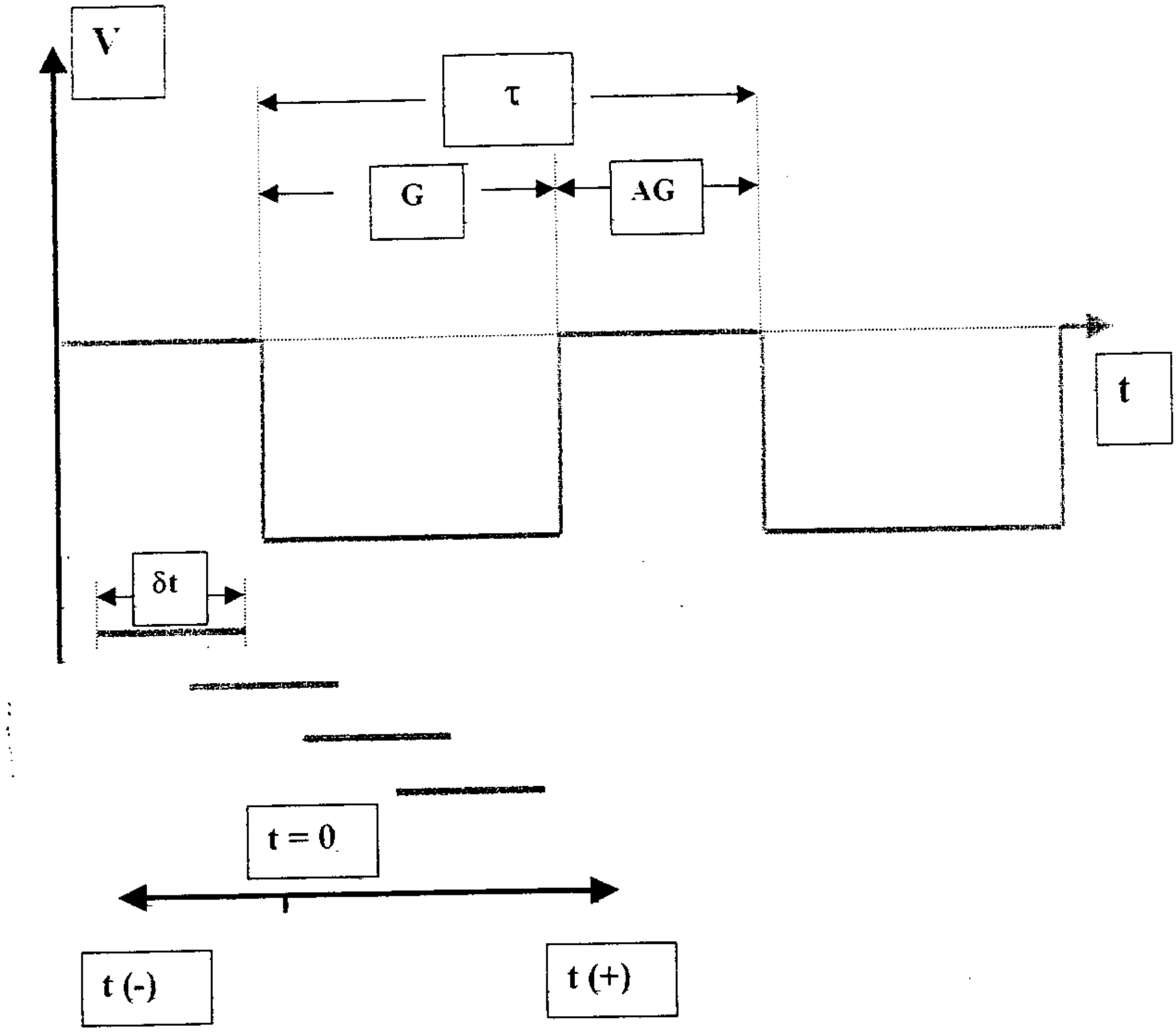
V
τ
G
AG
t
δt
t = 0
t (-)
t (+)

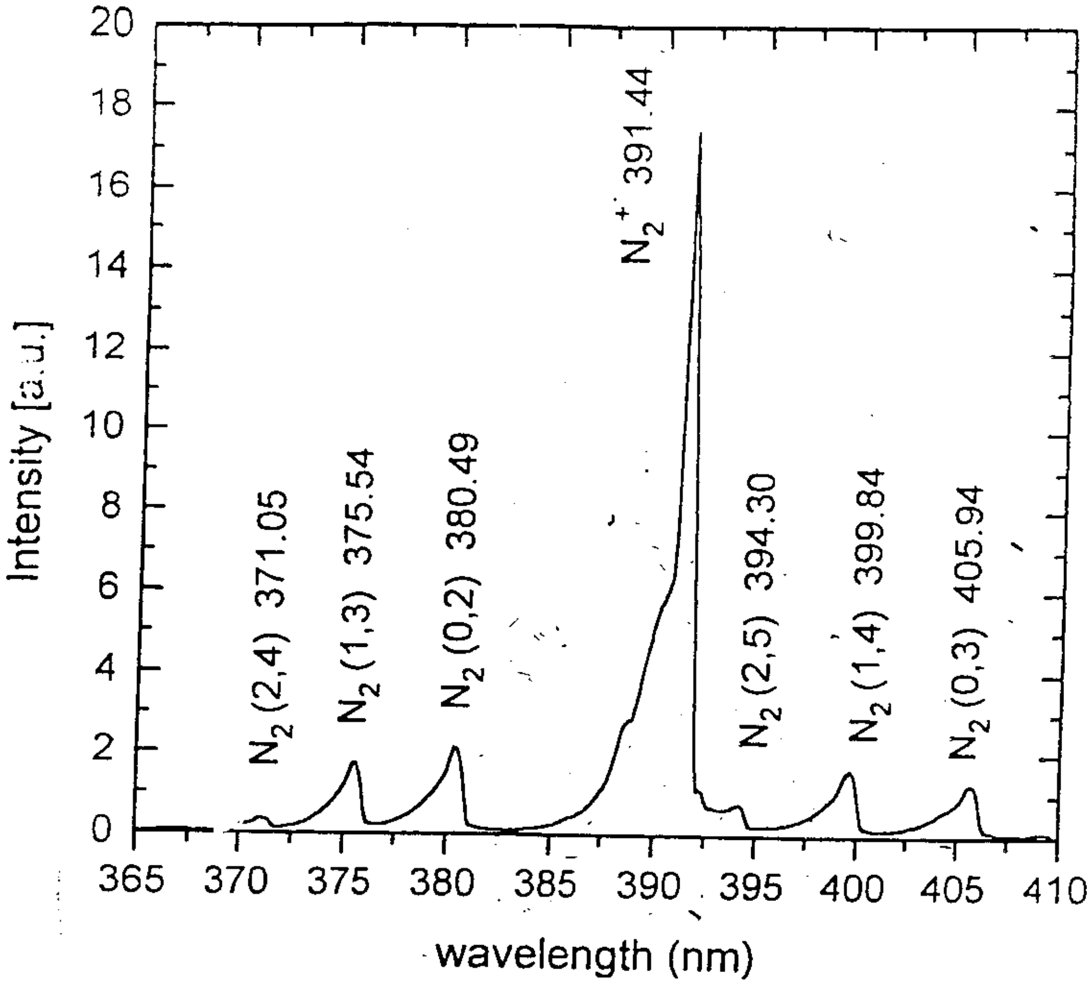
Intensity [a.u.]
wavelength (nm)
$N_2(2,4)$ 371.05
$N_2(1,3)$ 375.54
$N_2(0,2)$ 380.49
N_2^+ 391.44
$N_2(2,5)$ 394.30
$N_2(1,4)$ 399.84
$N_2(0,3)$ 405.94

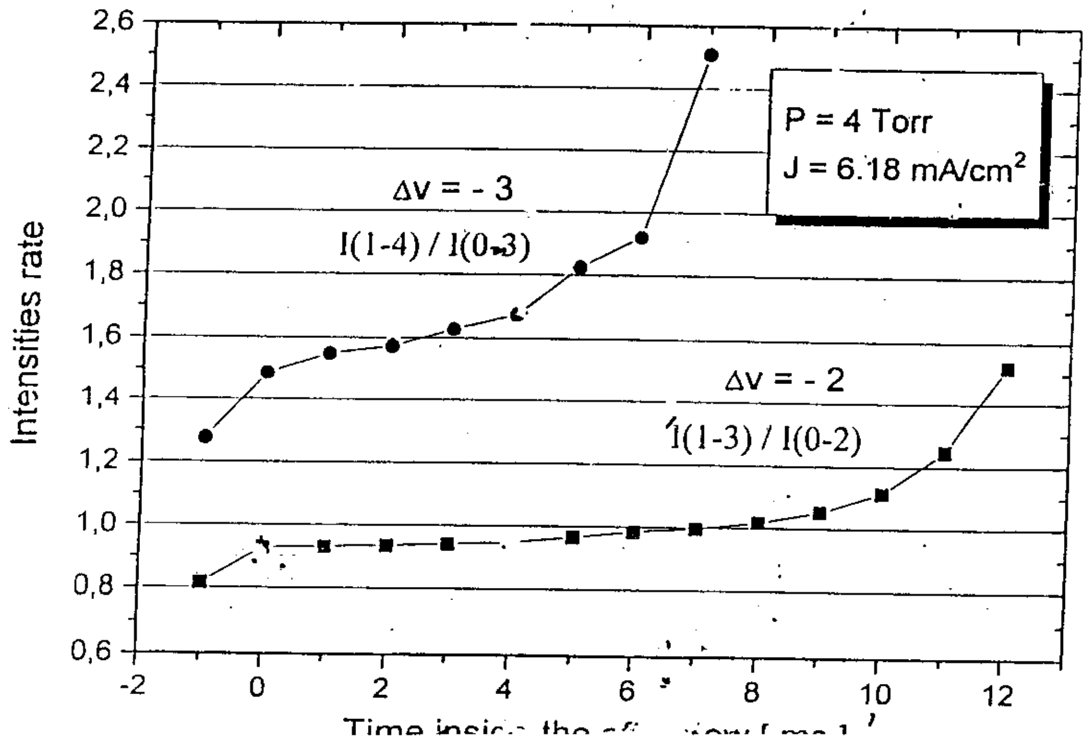
Intensities rate
P = 4 Torr
J = 6.18 mA/cm^2
Δv = - 3
I(1-4) / I(0-3)
Δv = - 2
I(1-3) / I(0-2)

$N_2^+(B,0\text{-}X,0)$ — **1st. negative**

$N_2(C,v'\text{-}B,v'')$ — $\Delta v=-2$ — **1st. positive**

$N_2(C,v'\text{-}B,v'')$ — $\Delta v=-3$ — **2nd. positive**

****

$$I_{CB}(v'-v'') = k(\lambda)[C, v]\, A_{CB}(v', v'') \,.\, \lambda^{-1}$$

* $N_2(C, v')$	**state density** $[C, v']$
* $k(\lambda)$	**spectral response of the instr.**
* A_{CB}	**radiative freq. of** $(C, v'\text{-}B, v'')$

****

$N_2(C, v')$ are produced by:

a) $e + N_2(X, v) \Rightarrow e + N_2(C, v')$

b) $N_2(A) + N_2(A) \Rightarrow N_2(C, v') + N_2(X)$

c) $N_2(A) + N_2(X, v{>}19) \Rightarrow N_2(C, v') + N_2(X)$

d) $N_2(X, v{>}24) + N_2(X, v{>}19) \Rightarrow N_2(C, v') + N_2(X)$

e) $e + N_2^+(X) \Rightarrow e + N_2^+($~~X~~ B$)$

f) $N_2(X, v{>}12) + N_2^+(X) \Rightarrow N_2(X, v) + N_2^+(B)$

****

When in a new cycle the glow begins:

g) $e + N_2(X, v) \Rightarrow 2e + N_2^+$

h) $e + N_2(X, v) \Rightarrow e + N + N$

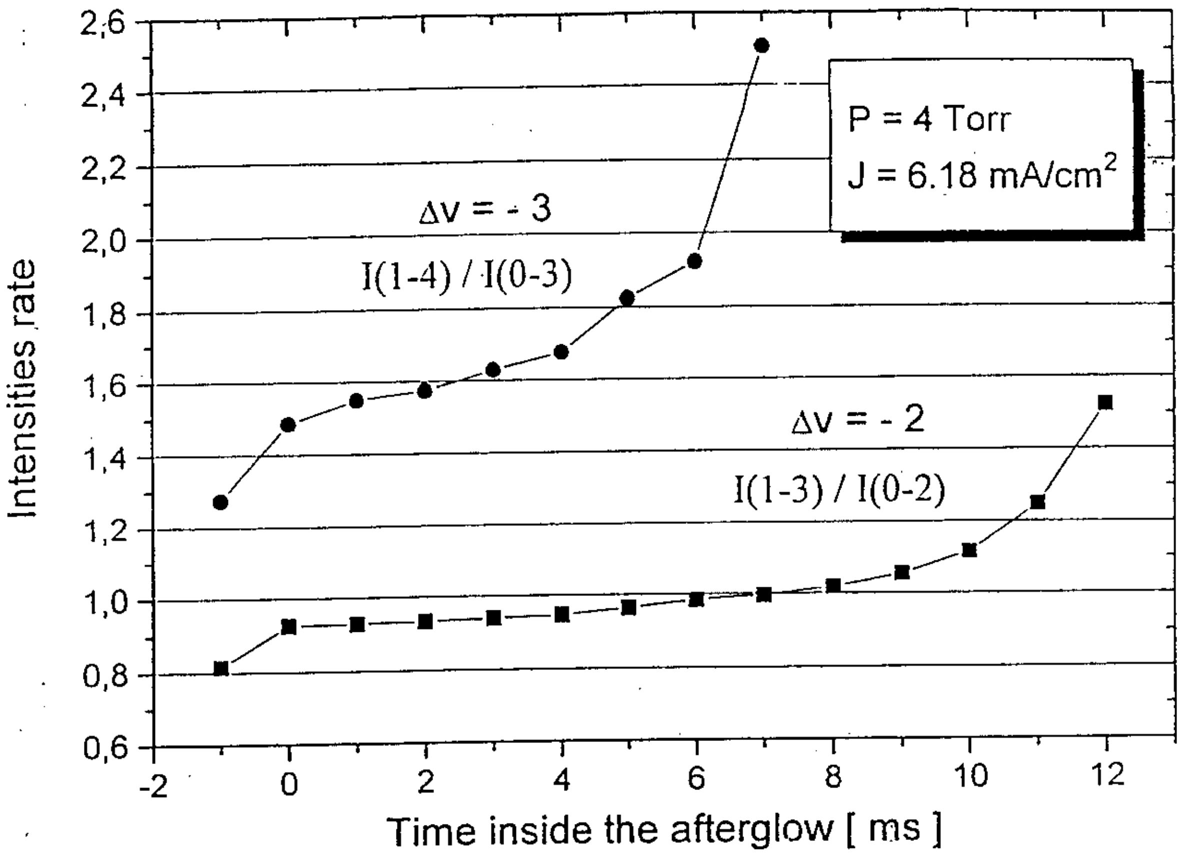
P = 4 Torr
J = 6.18 mA/cm2
Δv = - 3
I(1-4) / I(0-3)
Δv = - 2
I(1-3) / I(0-2)
Intensities rate
Time inside the afterglow [ms]

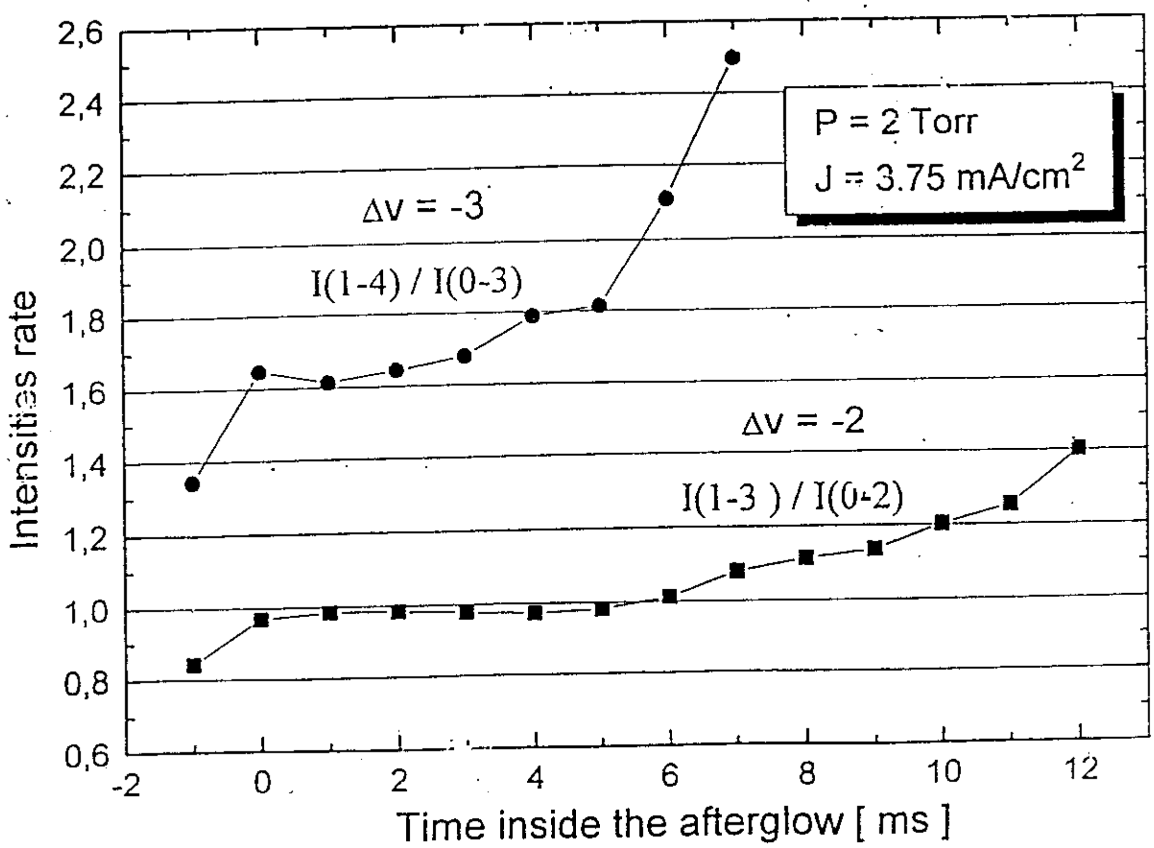
P = 2 Torr
J = 3.75 mA/cm2
Δv = -3
I(1-4) / I(0-3)
Δv = -2
I(1-3) / I(0-2)
Intensities rate
Time inside the afterglow [ms]

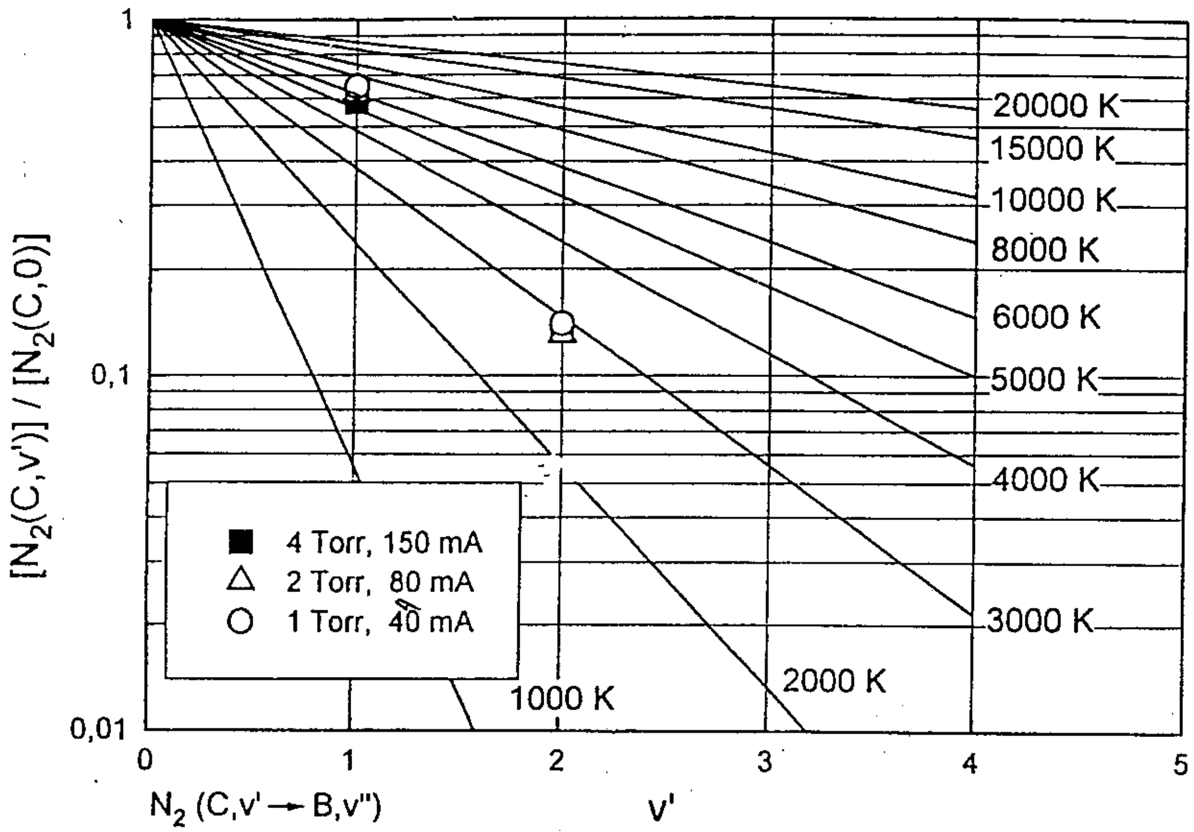

1
0,1
0,01
0
1
2
3
4
5
[N2(C,v')] / [N2(C,0)]
N2 (C,v' → B,v")
v'
20000 K
15000 K
10000 K
8000 K
6000 K
5000 K
4000 K
3000 K
2000 K
1000 K
4 Torr, 150 mA
2 Torr, 80 mA
1 Torr, 40 mA

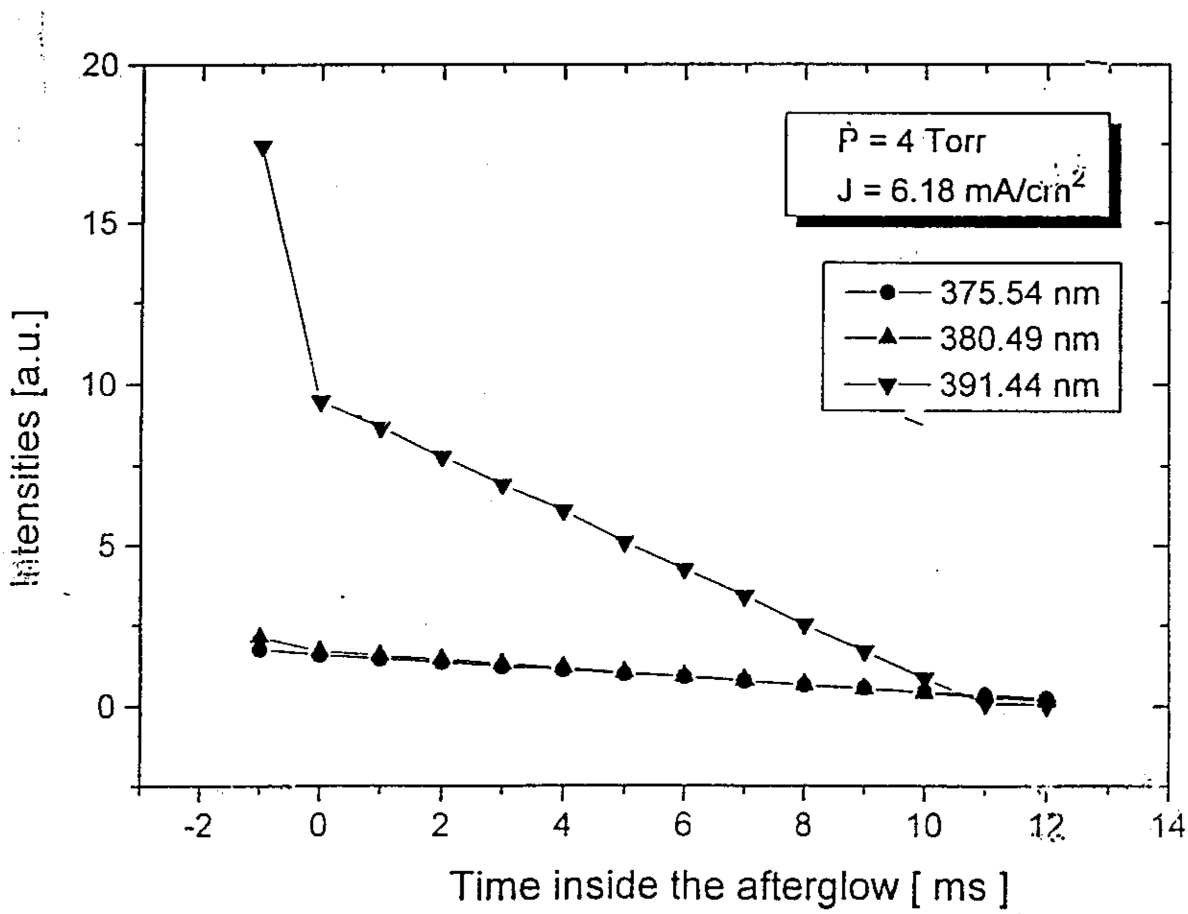

20
15
10
5
0
-2
0
2
4
6
8
10
12
14
Intensities [a.u.]
Time inside the afterglow [ms]
P = 4 Torr
J = 6.18 mA/cm2
375.54 nm
380.49 nm
391.44 nm

CONCLUSIONS

- Higher vibrational excitation of $N_2 (C, v' = 1)$ in the afterglow was observed.
- This increase can be explained by a decrese in the vibrational quenching of $N_2 (X, v)$ (neutral gas temperature decreasing).
- An increase in $N_2 (C, v' = 1)$ is related ~~with~~ to an increase in the $N_2 (X, v)$ vibrational population
- when a new discharge begins, the $N_2 (X, v)$ gives rise to N_2^+ and N production by eq. (g) and (h)

+ Maintenance voltage is lowered by the step-wise ionization process
  - power yield of the reactor increses
  - arcing process is reduced.

CONCLUSION II

The excitation of $N_2(C,v)$ and $N_2^+(B,0)$ has been analyzed by emission spectroscopy in negative glow of pulsed N_2-H_2 discharges and afterglows.

- For constant current discharge, the substrate temperature and operation voltage decreases when the H/N concentration ratio increases.
- In the afterglow the vibrational excitation of $N_2(C,v)$ increases, as happens for pure N_2 experiments and can be interpreted by collisions of $N_2(X,v)$ metastables molecules.
- For mixtures with H_2, although the $N_2(C,v')$ species are efficiently destroyed by H atoms, they are still sufficiently populated to excite the $N_2(C,v')$ vibrational states in the afterglow.

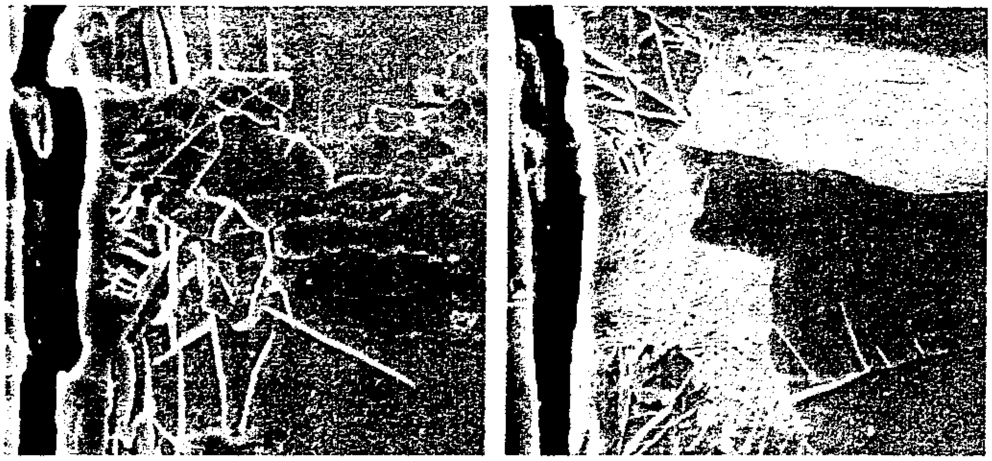

(a) 10μm (b) 10μm

Figure 4 Scanning electron micrograph of a transverse section adjacent to the treated face of the API 5L X-65 6h plasma nitrided steel showing that the intragranular acicular phase ($Fe_{16}N_2$) is present up to a depth of around 20μm.

3μm

Figure 5 Scanning electron micrograph of a transverse section adjacent to the treated face of the API 5L X-65 6h plasma nitrided steel showing, the interaction between the surface (γ'e ε) nitride layer and the cementite (Fe_3C) of a pearlite colony.

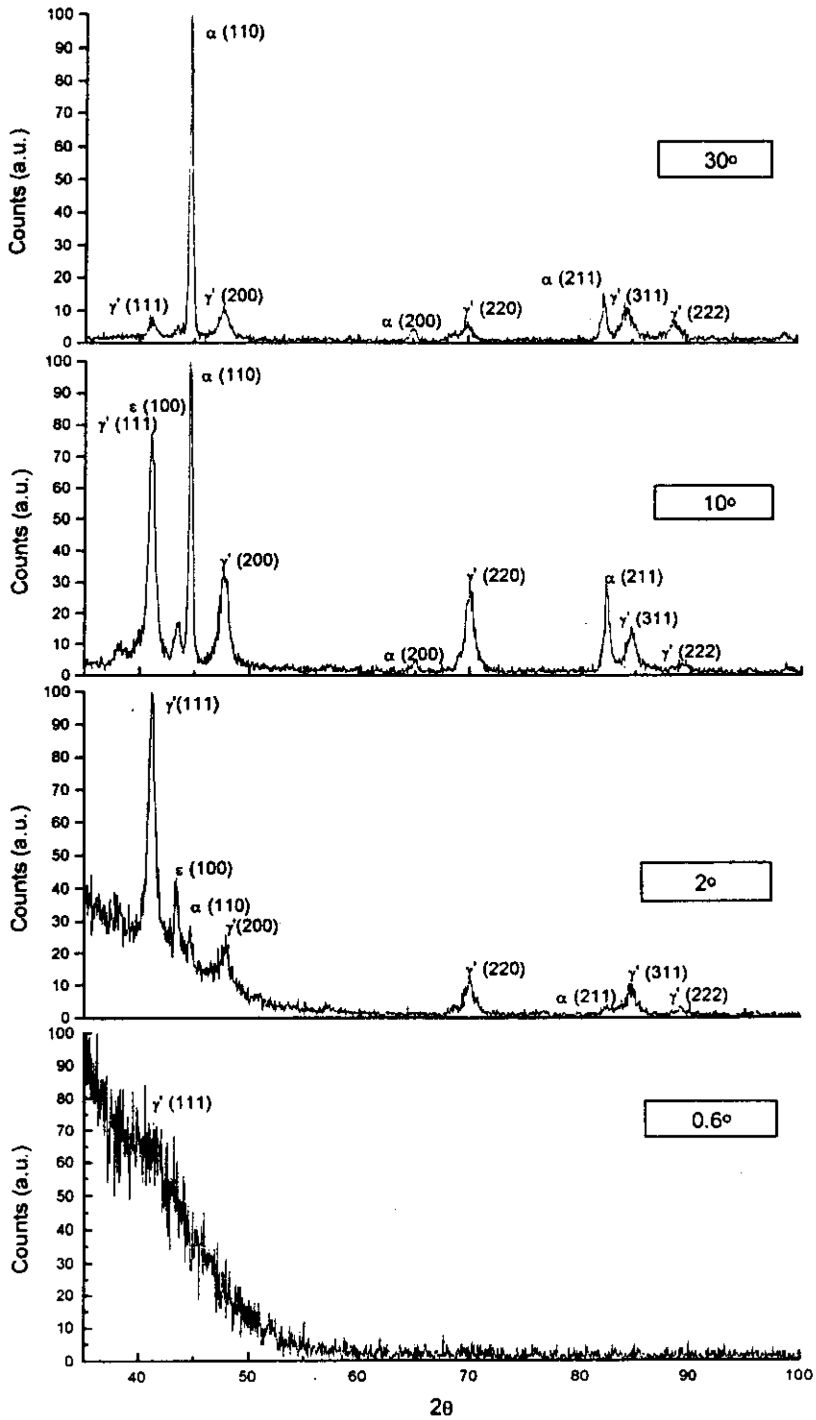

Figure 1 X-ray difractograms of the 6h plasma nitrided API 5L X-65 steel; for incident beam angles of; 0.6° , 2° , 10° and 30°

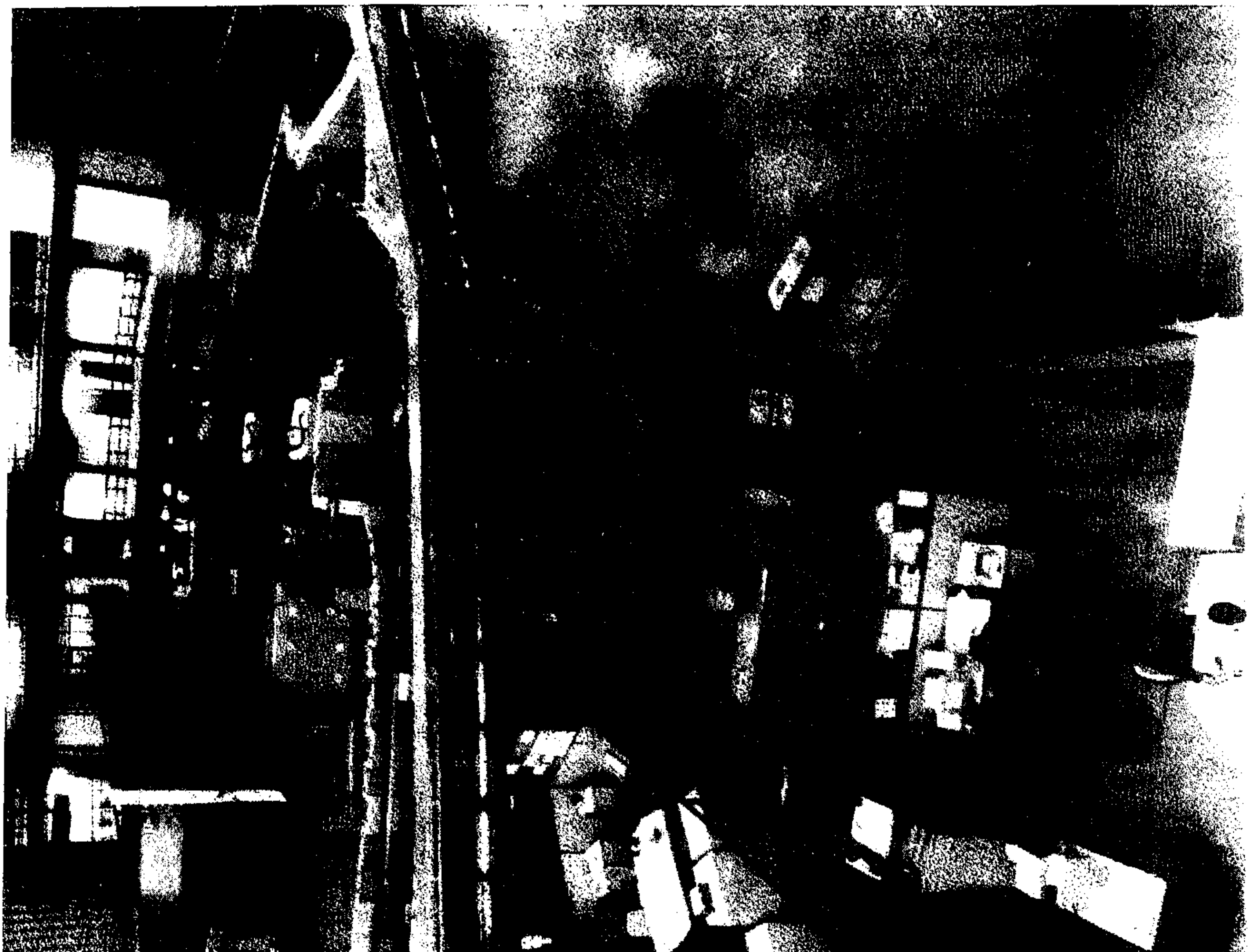

After-glow conditions

Electron temperature ≈ 0.5 eV

Eq. a): electronic threshold of ≈ 11 eV → eq. a) in the afterglow disappears.

$N_2(C)$ are produced by eq. b) → d)

$$\text{i)}\quad d\,[N_2(C,v')] / dt = [N_2(A)]^2\,k_b + [N_2(A)][N_2(x, v>19)]\,k_c + [N_2(x, v>24)]^2\,k_d - N_2(C)\,\nu'_c(v)$$

$N_2(A)$ are quickly destroyed by the walls

$N_2(x,v)$ are not, and are more populated than $N_2(A)$.

In equation i) the $[N_2(x, v>24)]^2\,k_d$ can explain the almost constancy of the $N_2(C)$ state ($d\,[N_2(C,v')] / dt = 0$)

The $N_2(x,v)$ high vibrational levels from the afterglow favor eq. g) and h) (at the beginning of the discharge in each cycle)

Low excitation threshold (2.5 eV) for the reaction e) may permit electronic excitation of $N_2^+(B)$ in the afterglow.

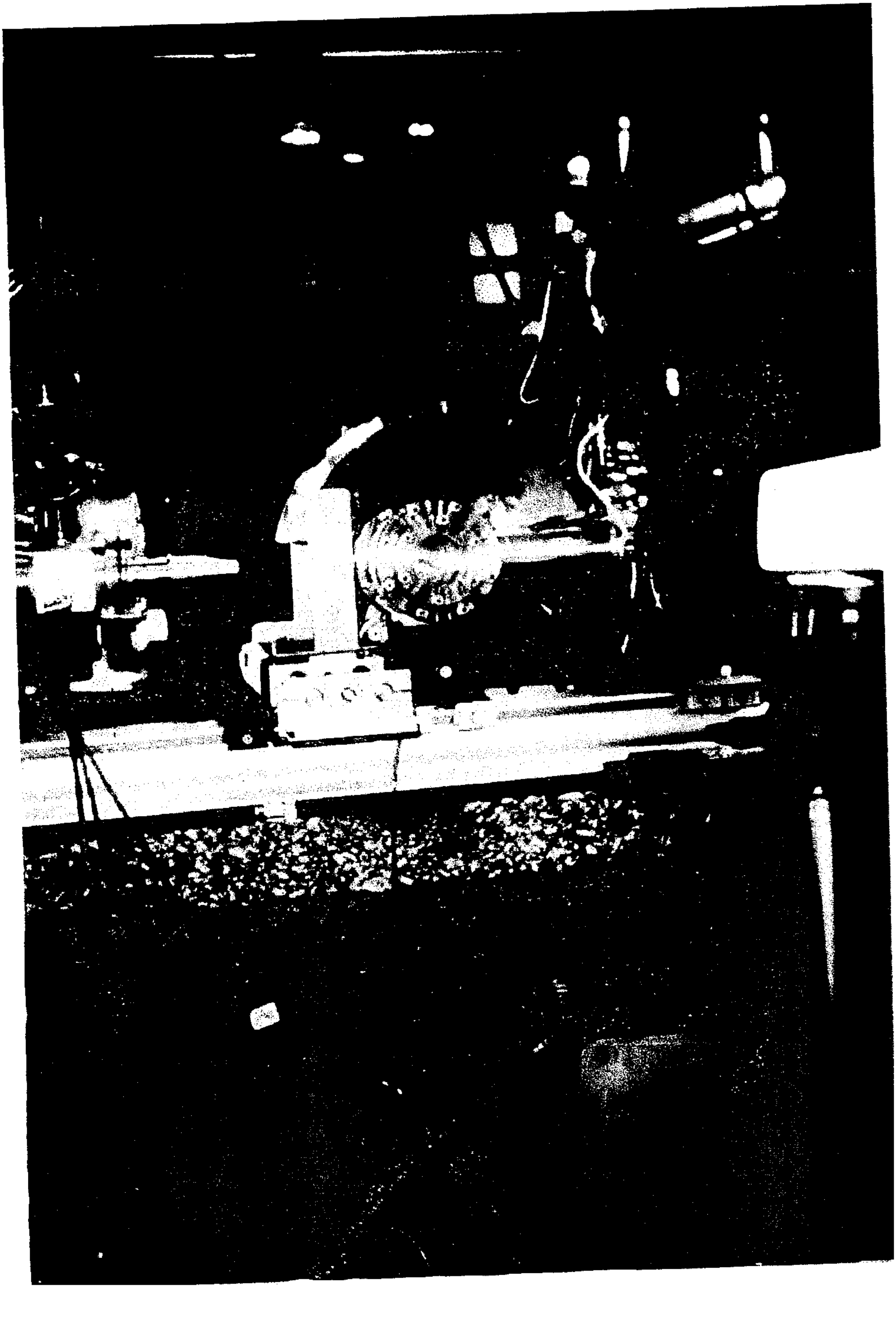

Table 1. Angular possition (Bragg angles) of the Fe_3N-ε (44.82°) and $Fe_{3.17}N_{0.83}$-ε phases for different treatment times

PHASES	2θ / d_{hkl} Å							
	a-1	a-2	a-3	a-4	a-5	a-6	...	a-13
Fe_3N (100)	------	------	43.77° *2.3609*	43.91° *2.3537*	44.98° *2.3005*	44.98° *2.3005*	...	43.91° *2.3537*
$Fe_{3.17}N_{0.83}$ (100)	------	------	44.82° *2.3083*	44.75° *2.3117*	44.89° *2.3049*	44.75° *2.3117*	...	44.68° *2.3152*
Fe_3N (101)	------	49.79° *2.0905*	49.93° *2.0850*	50.07° *2.0795*	50.14° *2.0768*	50.07° *2.0795*	...	50.14° *2.0768*
Fe_3N (102)	------	------	65.88° *1.6184*	66.02° *1.6153*	66.16° *1.6123*	66.16° *1.6123*	...	66.23° *1.6108*
$Fe_{3.17}N_{0.83}$ (102)	------	------	------	------	------	------	...	67.28° *1.5885*
Fe_3N (110)	------	------	80.08° *1.3679*	80.29° *1.3649*	80.36° *1.3639*	80.50° *1.3620*	...	80.50° *1.3620*

3.2.2- Hydrogen permeation modification of steel by surface ion nitriding

Using the same parameter of ion nitriding that the ones described in 3.2.2.1-, s[illegible] API 5L X-65 steel were treated for hydrogen permeation tests. The permeatio[illegible] performed in the Hydrogen Lab. of the Metallurgical Department of the Unive[illegible] [illegible]rogen [illegible]sults of Janeiro, Brazil.

Hydrogen permeation parameters were determined using elec[illegible]ng a TAI [illegible] the necessary cathodic charging potentials being ob[illegible] resistance [illegible] tests [illegible] all electrochemical tests [illegible]

C:\ARQ\saxe\T-

CONCLUSION III

The kinetic of phase development during ion nitriding with glow discharge was studied by In situ/Real Time/X ray diffraction, using Synchrotron radiation.

- The Fe-alpha phase peak intensity reduction during the process is a consequence of the formation of different iron nitrides at the top of the layer.
- The observed systematic increase in the interplanar distances during the first minutes of the process agree with the expected thermal expansion.
- There were observed the formation of three different nitrides: Fe_4N-gamma and Fe_3N-epsilon during the first minutes and $Fe_{3.17}N_{0,83}$ later on.
- During the process under isothermal conditions the interplanar spacing for all phases was constant, except for the Fe_3N one, that exhibit a decreasing trend probably due to the action of stresses.

↳ Célula de Permeação:

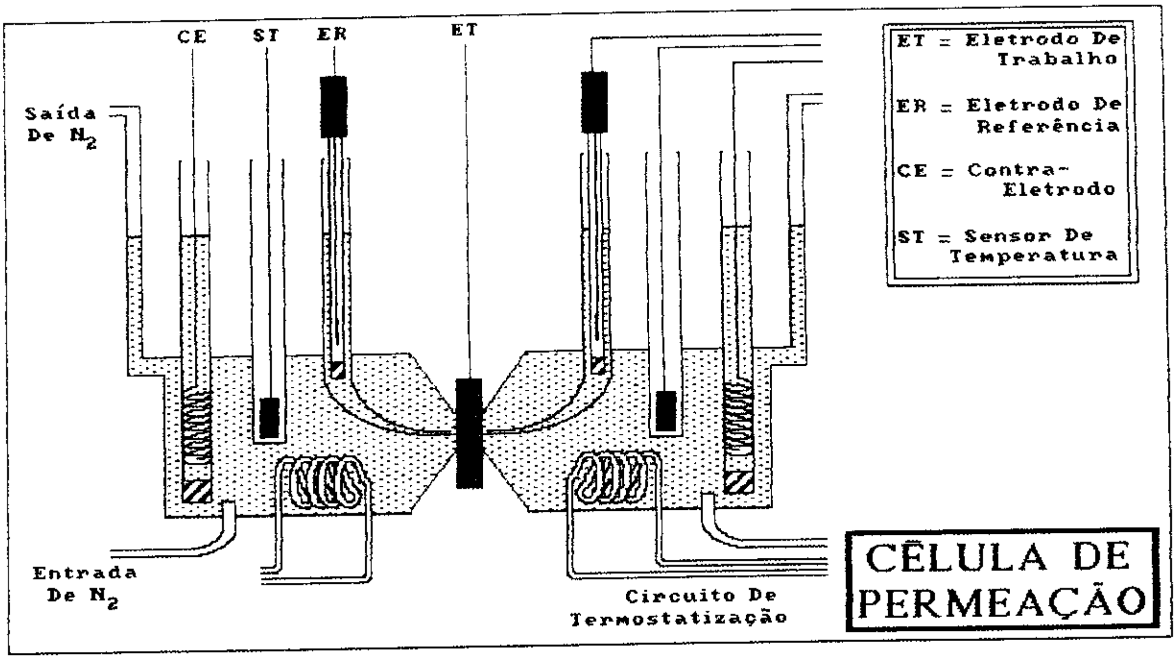

Figura 3.6.1- Diagrama esquemático da célula utilizada para testes eletroquímicos de permeação do hidrogênio.

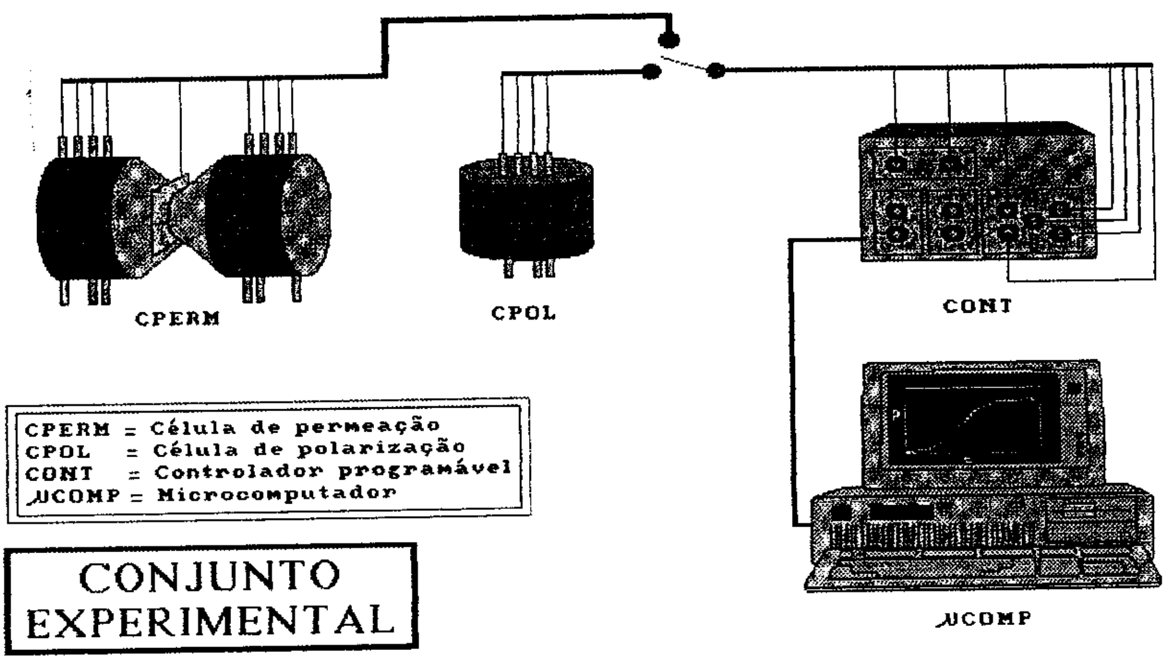

Figura 3.6.2- Diagrama esquemático da aparelhagem utilizada nos testes de permeação do hidrogênio

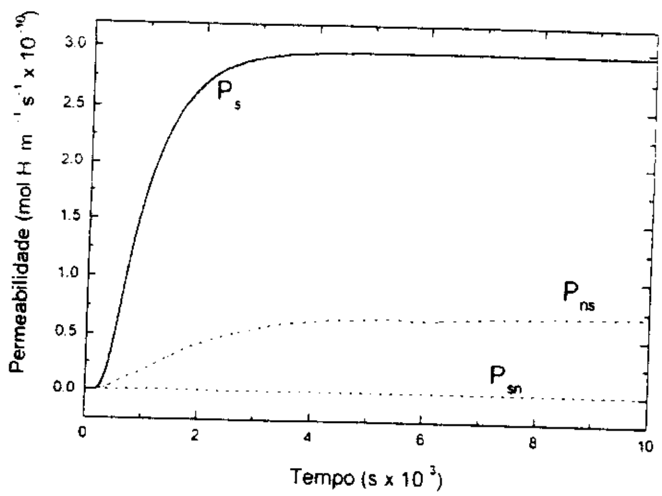

Figure 8 Hydrogen permeation curves for the API 5L X-65 steel; (PS) an untreated sample, (Pns) a 6h plasma nitrided sample tested with hydrogen generation at the nitrided face, (Psn) a 6h plasma nitrided sample tested with hydrogen generation at the non-treated face.

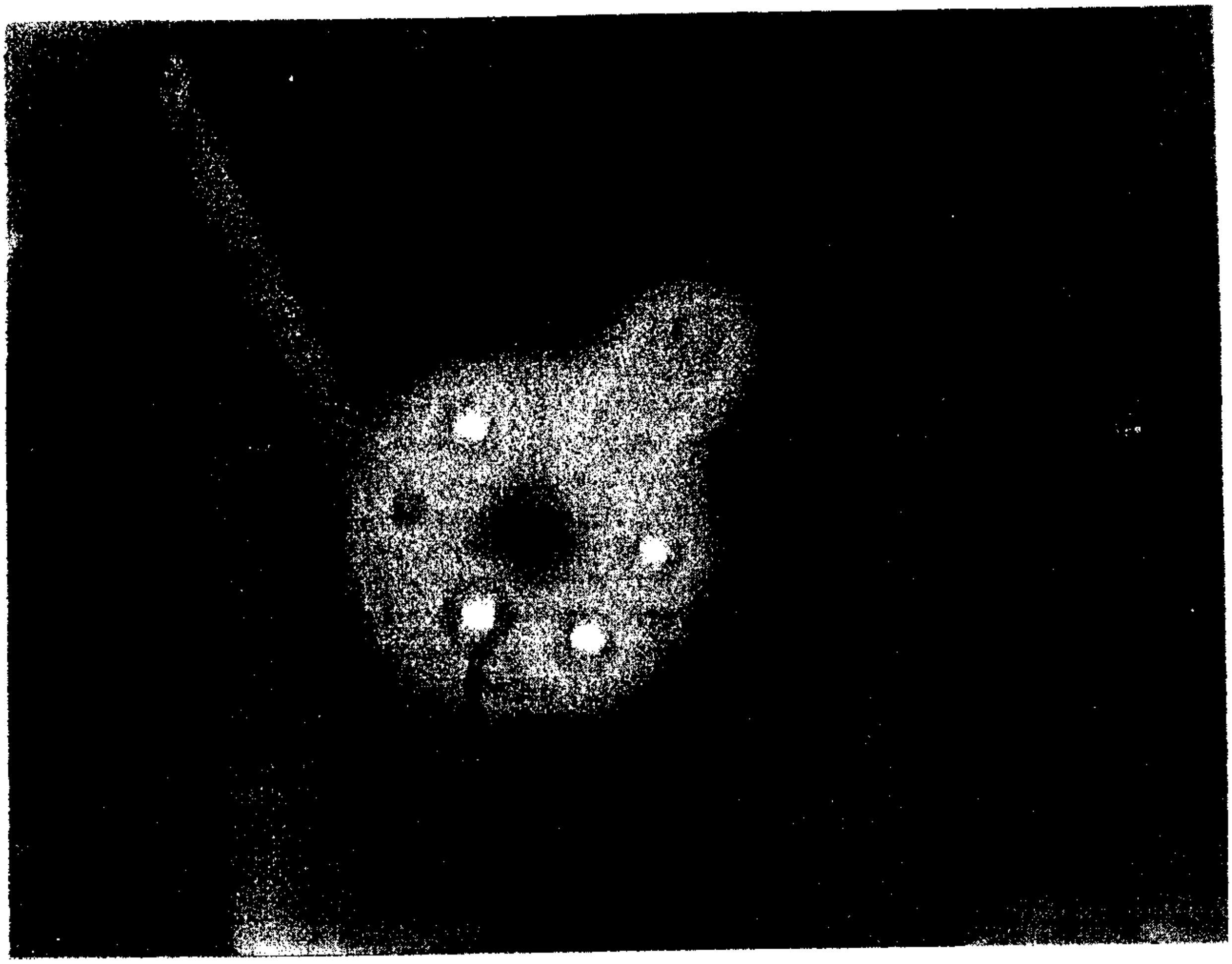

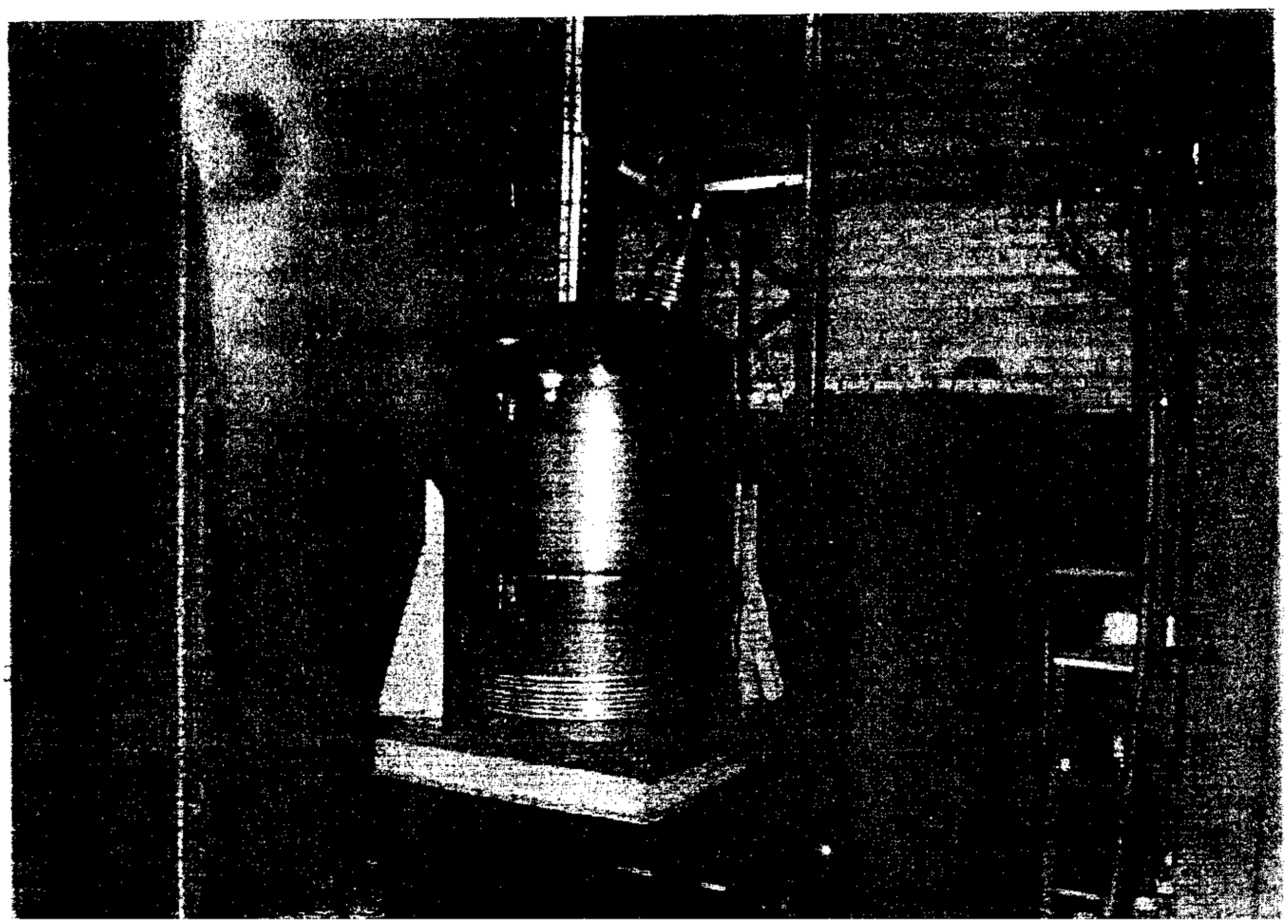

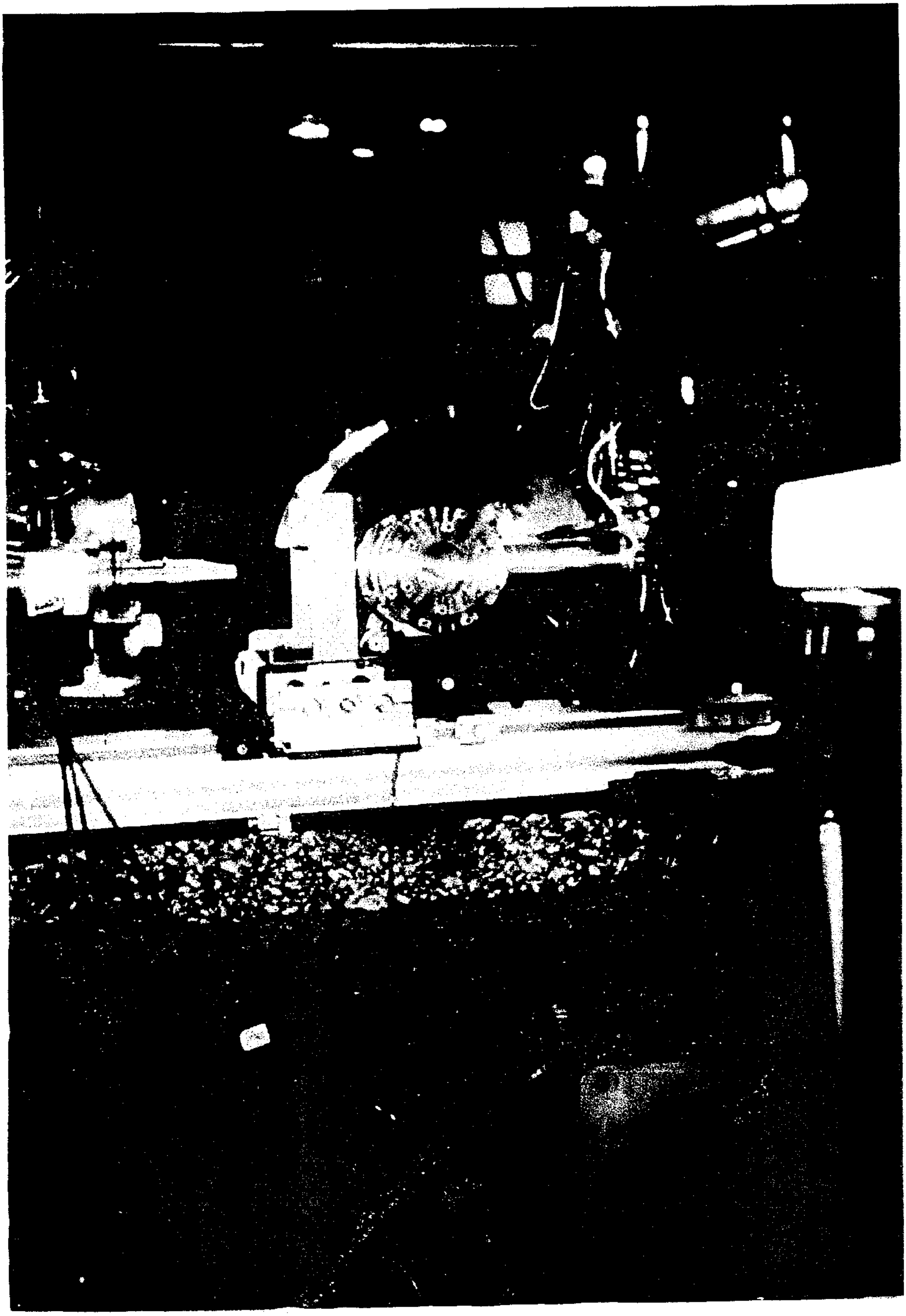

C:\ARQ\saxs\Jorge Feugeas\jorge13.gel , Range = 0.000-699.9 Counts, 100%

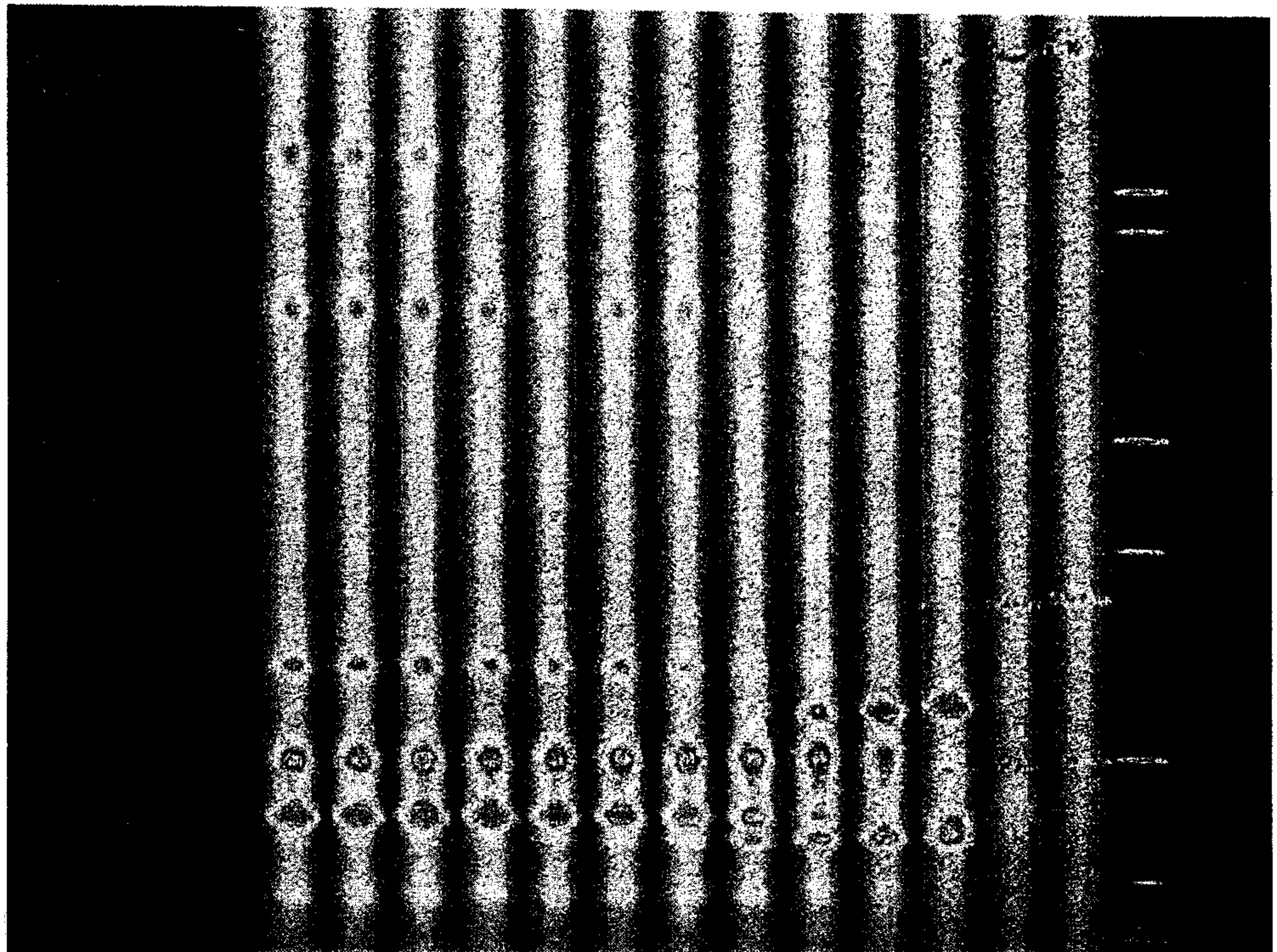

1010

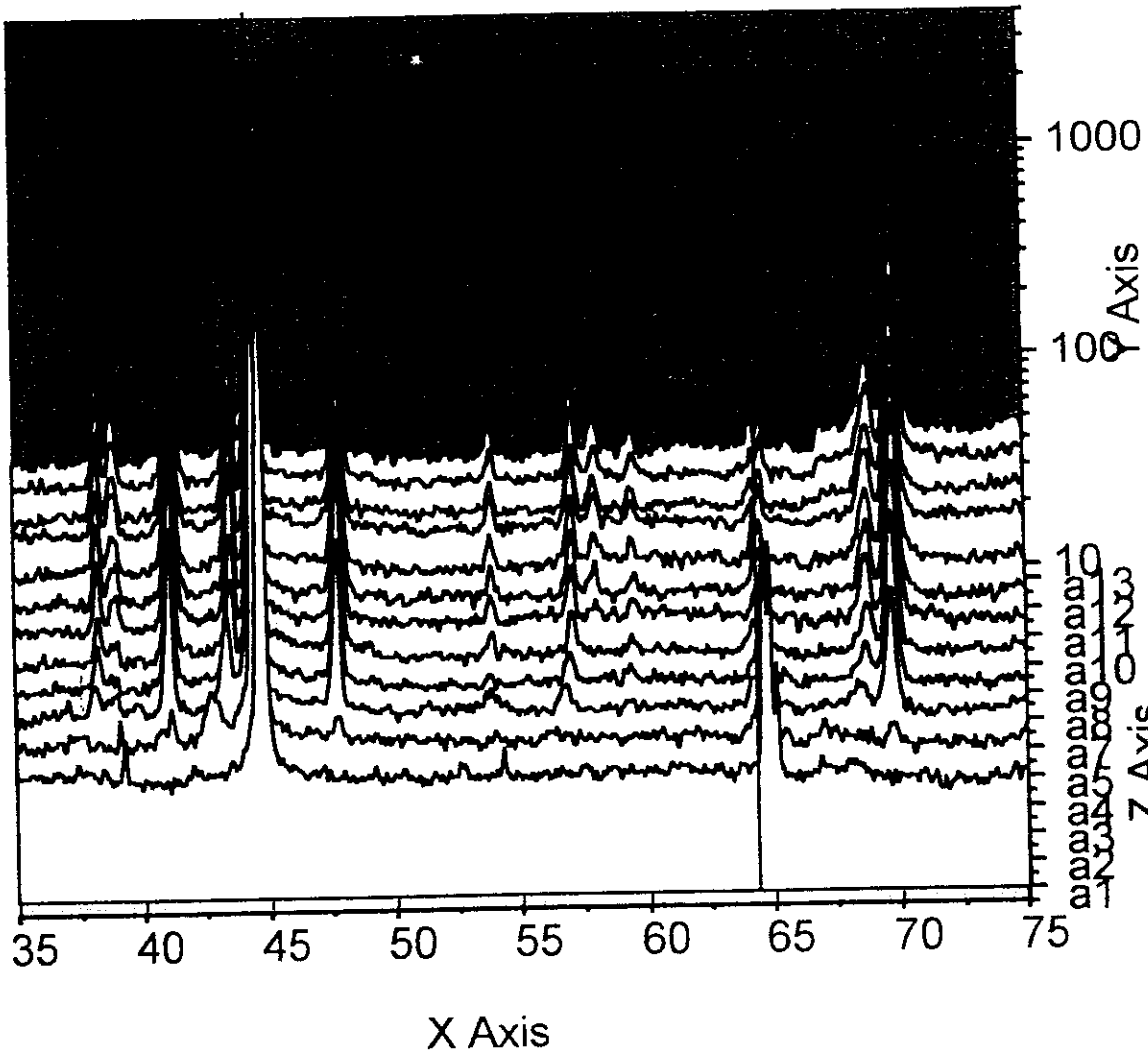
1000
100
10
Y Axis
Z Axis
a1
a2
a3
a4
a5
a6
a7
a8
a9
a10
a11
a12
a13
35
40
45
50
55
60
65
70
75
X Axis

Table I. Angular possition (Bragg angles) of the Fe_3N-ε (44.82°) and $Fe_{3.17}N_{0.83}$-ε phases for different treatment times

PHASES	2θ / d_{hkl} Å						
	a-1	a-2	a-3	a-4	a-5	a-6	...	a-13
Fe_3N (100)	------	------	43.77°	43.91°	44.98°	44.98°	...	43.91°
			2.3609	*2.3537*	*2.3005*	*2.3005*		*2.3537*
$Fe_{3.17}N_{0.83}$ (100)	------	------	44.82°	44.75°	44.89°	44.75°	...	44.68°
			2.3083	*2.3117*	*2.3049*	*2.3117*		*2.3152*
Fe_3N (101)	------	49.79°	49.93°	50.07°	50.14°	50.07°	...	50.14°
		2.0905	*2.0850*	*2.0795*	*2.0768*	*2.0795*		*2.0768*
Fe_3N (102)	------	------	65.88°	66.02°	66.16°	66.16°	...	66.23°
			1.6184	*1.6153*	*1.6123*	*1.6123*		*1.6108*
$Fe_{3.17}N_{0.83}$ (102)	------	------	------	------	------	------	...	67.28°
								1.5885
Fe_3N (110)	------	------	80.08°	80.29°	80.36°	80.50°	...	80.50°
			1.3679	*1.3649*	*1.3639*	*1.3620*		*1.3620*

3.2.2- Hydrogen permeation modification of steel by surface ion nitriding

Using the same parameter of ion nitriding that the ones described in 3.2.2.1-, samples of API 5L X-65 steel were treated for hydrogen permeation tests. The permeation tests were performed in the Hydrogen Lab. of the Metallurgical Department of the University of Rio de Janeiro, Brazil.

Hydrogen permeation parameters were determined using electrochemical hydrogen permeation tests, the necessary cathodic charging potentials being obtained from the results of prior potentiodynamic polarisation scans. All electrochemical tests were performed using a TAI GP-201H programmable electrochemical interface (galvanostat/potentiostat/zero resistance